

CHARLES UNIVERSITY

Faculty of Science

Study programme: Chemistry

Branch of study: Chemistry



Adéla Olšovská

The effect of reaction conditions and type of active sites on the kinetics of heterogeneously catalysed formylation of amines

Vliv reakčních podmínek a typu aktivních center na kinetiku heterogenně katalyzované formylace aminů

Bachelor thesis

Supervisor: Mgr. Ondřej Veselý

Consultant: Prof. Jiří Čejka

Declaration

I declare that I worked on this thesis solely by myself and that I cited all references used. This work or a substantial part of it was not used to obtain a different or the same academic degree.

In Prague, 17. 5. 2023

Adéla Olšovská

Acknowledgement

I would like to thank my supervisor Mgr. Ondřej Veselý for his guidance, unceasing support and patience, as well as my consultants Prof. Jiří Čejka and Ing. Jan Přeč, Ph.D. for their valuable opinions and advice. My thanks also belong to the members of Synthesis, Catalysis and Advanced Materials research group for introducing me to various characterisation methods and for helping me with measurements, including nitrogen adsorption (Mgr. Martin Kubů, Ph.D.), and infrared spectroscopy (Mgr. Maria Shamzhy, Ph.D. and Kinga Gołębek, Ph.D.).

Abstract

Formamides are valuable compounds in pharmaceutical production and organic synthesis; however, their common synthesis methods suffer from number of drawbacks including low reaction rate and contamination with heavy metals leached from a catalyst. According to several articles, these problems could be overcome by using zeolite-based catalysts. Nevertheless, the mentioned articles provide somewhat conflicting results and also lack a clear description of which centres in zeolites are catalytic active.

Therefore, we prepared a set of zeolite-based catalysts commonly described in the literature (zeolite Beta ion exchanged to H^+ and Cu^{2+} form) in order to test them as catalysts and clarify their catalytic behaviour and nature of the active sites. We chose formylation of N-methylaniline by formic acid as the model reaction for our research and performed a series of experiments under varying conditions (solvents, concentration of reactants, temperature). In contrast to the published articles, none of the investigated materials demonstrated significant catalytic activity in our experiments. Moreover, we found that the often pronounced catalyst: zeolite Beta ion-exchanged into the copper form, is unstable in the presence of formic acid, which causes leaching of copper into the reaction mixture. At the same time, we were able to prove that the reaction proceeds spontaneously in 1,4-dioxane in the absence of a catalyst and with up to 98% selectivity. Hence the question arises, whether the catalysis is even necessary to carry out this reaction.

Moreover, we found a significant dependence of the rate of uncatalysed reaction on external conditions such as ambient temperature. In light of this discovery, we have to express a concern that the authors of the published articles may not have been aware of the spontaneous course of the reaction in the collected samples and that the results presented in the literature may be greatly distorted and inconsistent with reality.

Keywords: formylation, zeolites, formamides, Beta zeolite, acid catalysis

Abstrakt

Formamidy jsou cenné sloučeniny pro farmaceutickou výrobu a organickou syntézu. Běžné metody jejich syntézy však mají řadu nevýhod, včetně nízké reakční rychlosti a kontaminace těžkými kovy vyluhovanými z katalyzátoru. Podle několika článků by tyto problémy mohly být překonány použitím katalyzátorů na bázi zeolitů. Nicméně uvedené články poskytují poněkud rozporuplné výsledky, a také postrádají jasný popis toho, která centra v zeolitech jsou katalyticky aktivní.

Proto jsme připravili soubor katalyzátorů na bázi zeolitů běžně popisovaných v literatuře (zeolit Beta iontově vyměněný do H^+ a Cu^{2+} formy), abychom je otestovali a objasnili jejich katalytické chování a povahu aktivních míst. Jako modelovou reakci pro náš výzkum jsme zvolili formylaci N-methylanilinu kyselinou mravenčí a provedli jsme řadu experimentů za různých podmínek (rozpuštědla, koncentrace reaktantů, teplota). Na rozdíl od publikovaných článků, žádný ze zkoumaných materiálů nevykazoval v našich experimentech významnou katalytickou aktivitu. Navíc jsme zjistili, že zeolit Beta iontově vyměněný do formy mědi, který je v literatuře zmiňován nejčastěji, je v přítomnosti kyseliny mravenčí nestabilní, což způsobuje vyplavování mědi do reakční směsi. Zároveň se nám podařilo prokázat, že reakce probíhá spontánně v 1,4-dioxanu bez katalyzátoru a až s 98% selektivitou. Vystává tedy otázka, zda je k provedení této reakce katalýza vůbec nutná.

Navíc jsme zjistili, že i mírná změna pokojové teploty má zásadní vliv na průběh reakce. Ve světle tohoto zjištění musíme vyjádřit obavu, že autoři publikovaných článků si nemuseli být vědomi spontánního průběhu reakce v odebraných vzorcích, a že výsledky prezentované v literatuře mohou být značně zkreslené a neodpovídající skutečnosti.

Klíčová slova: formylace, zeolity, formamidy, Beta zeolit, kyselá katalýza

Contents

1	Introduction.....	6
2	Thesis goals.....	7
3	Theoretical Part.....	8
3.1	Zeolites.....	8
3.1.1	History	8
3.1.2	Structures	9
3.1.3	Properties	10
3.1.4	Synthesis.....	11
3.1.5	Characterisation	12
3.2	Catalysis	16
3.2.1	Homogeneous and heterogeneous catalysis	17
3.2.2	Mechanisms and principles.....	17
3.2.3	Evaluation of the catalytic experiment	18
3.2.4	Zeolites in catalysis.....	20
3.3	Formylation.....	21
3.3.1	Mechanism	21
3.3.2	Formylation over zeolites.....	22
4	Experimental Part.....	23
4.1	List of used chemicals	23
4.2	Synthesis of Beta zeolites	23
4.3	Characterisation of Beta zeolites.....	24
4.4	Catalytic experiments	25
5	Results and discussion.....	27
5.1	Synthesis and characterisation of catalysts.....	27
5.2	Catalytic experiments	30
6	Conclusion	38
7	References.....	40

1 Introduction

Formamides are valuable compounds and intermediates in organic synthesis. Formamides and their derivatives find application as fungicides, reagents for synthesis of pharmaceutical compounds (e.g. cancer cell growth inhibitory constituents ¹) or as reagents in Vilsmeier formylation reaction. ² Last but not least, due to their Lewis basic character they catalyse a number of chemical reactions such as allylation and hydrosilylation of carbonyl compounds. ^{3,4}

Formylation commonly involves acid, organic or transition metal catalysts and the use of stoichiometric amounts of formylating agents (e.g. formic acid, chloral, formaldehyde). ^{3,5} However, these reagents come with drawbacks such as formation of by-products, or low product yields. Furthermore, separating homogeneous catalysts from the reaction mixture tends to be challenging which makes them unsuitable for large-scale processes. ⁶ On top of that, transition metal catalysts possess a risk of contaminating the product with heavy metals. This makes these catalysts unsuitable for synthesis of pharmaceutical compounds. ⁴

Heterogeneous catalysts, such as zeolites, currently dominate the chemical industry. Their main benefits include their stability, low cost, easy-separation, reusability, application in flow systems, and environmental tolerance. They catalyse key processes such as fluid catalytic cracking, hydrocracking or xylene isomerisation. In my work, I studied the application of zeolites as catalysts for formylation of amines. ⁷

2 Thesis goals

This thesis aimed to verify and assess the concept of formylation of amines over zeolite based catalysts published in the literature. We set the following goals:

- Prepare a set of Beta zeolites with different active sites (i.e. H^+ and Cu^{2+})
 - Characterise their crystallinity, textural properties and type, strength and concentration of acid sites
- Find suitable conditions for formylation of N-methylaniline (e.g. solvent/solvent-free, concentration)
- Describe the type of active sites in each catalyst and determine their role in catalysing the formylation
 - Describe the relation between active site type and reactant conversion, product selectivity and catalyst stability
- Investigate the catalyst stability and reusability in the reaction

3 Theoretical Part

3.1 Zeolites

Zeolites are crystalline microporous aluminosilicates which possess large surface areas, pore volumes, acidity, ion exchange ability and chemical and thermal stability.⁷ Zeolites participate as acid catalysts in numerous key industrial processes including petroleum cracking and hydrocracking, biomass conversion, production of phenol by hydroxylation, ethylbenzene and cumene by alkylation and propylene oxide by epoxidation.^{8,9,10} Zeolites are also widely used as environmentally friendly water softeners in laundry detergents.¹¹

3.1.1 History

The name “zeolite” originates from Greek words “zeo”, meaning boil, and “lithos”, meaning stone. The name was firstly used in 1756 by Swedish mineralogist Axel Crønsted who observed that zeolites released steam upon heating, which was caused by the evaporation of water adsorbed inside their pores.¹²

Zeolites attracted more interest in the 19th century when Saint-Claire-Deville published the first report on the hydrothermal synthesis of zeolites.¹³ However, the limited methods for characterisation of materials hindered further research. The discovery of X-ray diffraction (XRD) in 20th century enabled analysis of crystal structure and thereby accelerated the development of synthetic methods for zeolites.¹³

In the 1961, R. M. Barrer and P. J. Denny prepared the first zeolite using an organic molecule, tetramethylammonium hydroxide (TMA-OH), as a template in their reaction mixture.¹⁴ This approach enabled a higher degree of control over the zeolite topology and chemical composition. It is used up-to-now in the majority of zeolite synthesis e.g. synthesis of Beta uses tetraethylammonium hydroxide (TEA-OH)¹⁵ and synthesis of ZSM-5 tetrapropylammonium hydroxide (TPA-OH).¹⁶

In 1960s zeolites have found applications as catalysts in various petrochemical and chemical processes, especially in hydrocracking, thanks to their shape-selectivity. Since then, zeolites are commonly used in catalytic cracking and hydrocracking of oil, to enhance the

selectivity towards desired chemicals and fuels in larger quantities, to synthesise xylenes, ethylbenzene, PET, gasoline and light olefins from methanol etc.¹⁷

Early 1980s, zeolite-related materials like alumino- and gallo-phosphates or titanosilicates were discovered. These materials have considerable compositional diversity and they introduce a number of heteroatoms, resulting in completely different properties and possibilities of use compared to common zeolites. Recent research aims at developing chiral frameworks and extra-large pore zeolites, which could catalyse formation of bulky organic compounds.^{18,19}

3.1.2 Structures

Zeolites are microporous materials which means they contain pores with diameter from 0.5 to 1.5 nm.²⁰ Zeolite structure comprises of tetrahedral TO_4 units with the T atom in the centre. The tetrahedra are linked via oxygen atoms in the corners to form the three-dimensional crystalline framework.²¹ International zeolite association (IZA) recognizes more than 250 different frameworks to this day.²² We distinguish the zeolites based on the size of their pores (number of tetrahedrons that create the rings) as: small-pore (8-ring pores), medium-pore (10-ring pores), large-pore (12-ring pores) or extra-large pore (≥ 14 -rings).²³ Another important characteristic of zeolites is their pore dimensionality. Pore networks could be one-, two- or three-dimensional according to the direction and connectivity of the channels.²⁴

The majority of zeolites are aluminosilicates; however, the zeolite framework may also contain different tetravalent (e.g. Ge^{4+} , Sn^{4+} , Ti^{4+}), or other trivalent (e.g., B^{3+} , Ga^{3+} , Fe^{3+}) heteroatoms in framework positions. The incorporation of trivalent atoms introduces negative charge into the framework.^{25, 26} The negative charge then needs to be compensated by cations such as H^+ , Na^+ , NH_4^+ or transition metal cations in extra-framework positions.²⁷ The H^+ cations form Si-(OH)-Al bridges, which provide the zeolite with Brønsted acidity.

3.1.3 Properties

Metallosilicate zeolites behave as solid **acids**. They can exhibit both Brønsted and Lewis acidity. Brønsted acid sites originate from the presence of H^+ cations which compensate negatively charged framework sites, typically aluminium. Lewis acid sites originate from elements with vacant electron orbital (e.g. Sn, Ge, Ti, Zr,) located in the zeolite framework, or from metal cations that were introduced to the zeolite via ion exchange.^{25, 28} Acidity of zeolites could also change as a result of post-synthetic treatment such as calcination. Calcination of zeolites at high temperatures causes dehydroxylation of the structure. Hence, the dehydrated Brønsted sites transform to Lewis sites (Figure 1).^{29, 30, 31, 32}

For instance, zeolite Beta contains both Brønsted sites and Lewis sites, thanks to the presence of Al atoms. Their relative concentration depends on the temperature used during the calcination and length of the procedure. According to *Kunkeler et al.* zeolites Beta calcined at 450 °C for 30 minutes in dry atmosphere had both Brønsted and Lewis sites, whilst Beta calcined at 550 °C for 3 days in wet atmosphere had almost exclusively Lewis sites. The catalytic capabilities of the samples were also verified in reaction of 4-tert-butylcyclohexanone, which in case of longer activation times led to significantly higher conversions due to the higher concentration of Lewis acid sites present in the catalyst.³³

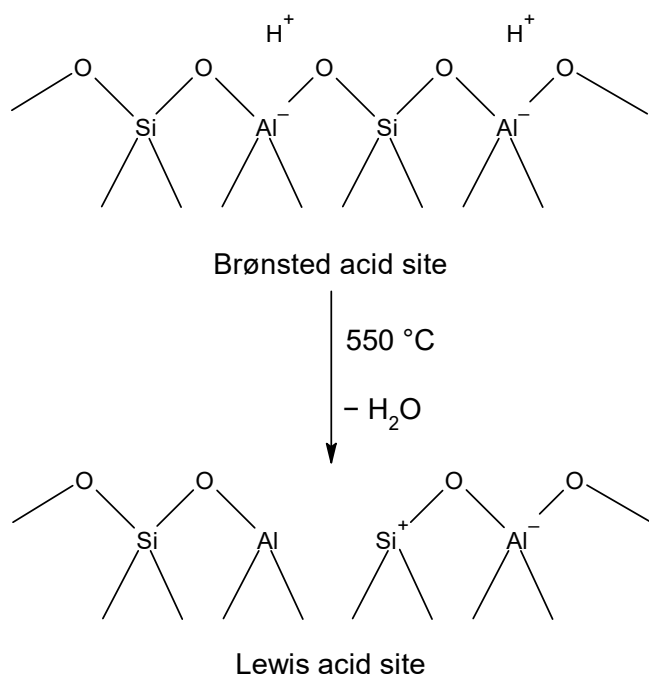


Figure 1: Dehydration of Brønsted acid site to a Lewis acid site

Zeolites contain **uniform micropores** in their crystal structure. Structural units, such as rings or cavities, determine the size and geometry of the pores. The pores can restrict molecules that enter/exit the channel system based on their kinetic diameter.^{34, 35} This effect especially manifests in selectivity towards reactants, products or transition states with more suitable geometry during catalytic reactions.⁹ For example alkylation of toluene in the absence of zeolites provides mixture with 25 % of p-xylene corresponding to the thermodynamic equilibrium.³⁶ In contrast, alkylation catalysed by modified HZSM-5 zeolite produces mixture with up to 98 % of para isomer. The para isomer is less sterically hindered while the other isomers are retained in the narrow pores of the zeolite, which favours the production of p-xylene as a major product. In other words, **shape-selectivity** depends on the structure of the zeolite and shifts the equilibrium of the reaction in favour of p-xylene as a product.³⁷

Chemical and thermal **stability** even under severe reaction conditions is another significant benefit of zeolites. Stability is one of the key reasons why zeolites are commonly used in industry. The stability of zeolites enables their repeated use, which is economically convenient. Also, their chemical stability makes them environmentally friendly in contrast to acids such as H₂SO₄ or AlCl₃.^{23, 28}

3.1.4 Synthesis

Zeolites are commonly synthesised using the hydrothermal method. Typical synthesis mixture consists of sources of Si and Al (or other heteroatoms) dissolved in a basic solution of water, ethanol or ionic liquid, sealed in an autoclave. The crystallisation conditions of the zeolite involve elevated temperature (100-200 °C) and high pressure (>1 bar). The duration of hydrothermal crystallisation varies depending on the temperature and desired product (type of zeolite, particle size), typically from several hours, days up to even weeks.³⁸ Depending on the amount of aluminium in the zeolite structure, the concentration of acid centres changes accordingly.¹²

Majority of zeolite synthesis procedures include addition of organic **structure directing agents** (SDAs) in the synthesis mixture (eg. tetraethylammonium, tetrapropylammonium and tetrabutylammonium cations). The SDAs promote formation and stabilisation of certain

building units and framework types.³⁹ Larger SDAs tend to stabilise frameworks with large cavities, however, no straightforward relationship between SDA structure and framework topology has been found. In rare cases, SDAs could act as true templates, meaning that structure arises around them and pores are formed with corresponding shape and size.^{19,40}

Molar ratio of Si and Al influences phase selectivity and time of crystallisation. Most zeolites crystallise within a defined range of Si/Al ratios. For example: zeolite ZSM-12 crystallises commonly at ratios Si/Al > 30. In case of lower Si/Al, the synthesis also produces an impurity phase, different zeolite – Beta, zeolite ZSM-5 or an amorphous phase.⁴¹ The Si/Al can also impact the synthesis time. Synthesis of zeolite Beta proceeds the fastest when Si/Al ratio is about 50. **Stirring** of the synthesis mixture of zeolite Beta during crystallisation leads to a shorter induction period and overall shorter crystallisation time. Lower **water content** in synthesis mixture increases **alkalinity of synthesis gel** which shortens induction period and accelerates crystallisation. However, it also leads to lower average crystal size. At the same time the increased pH of the synthesis gel causes the resulting crystals to have slightly higher Si/Al ratio.^{42,43}

Higher **temperature** generally fastens crystallisation and shortens synthesis time. However, higher temperatures can also change the phase selectivity and another zeolite structure can form. In essence, each zeolite can form in a defined range of temperatures and time.⁴³

Last but not least, it is worth mentioning that several mechanisms of nucleation and crystallisation of zeolites were proposed, however, the detailed mechanism of synthesis is still unknown and the attempts to understand every step in zeolites' formation are on-going.^{7,38}

3.1.5 Characterisation

The catalytic performance of a zeolite depends on a number of key properties including framework topology; textural properties (i.e. external surface, pore size), type, concentration and strength of acid sites. It is essential to properly characterise these

properties in order to study the catalytic behaviour of the material. In my work, following methods were used in order to obtain the characterization.

Powder X-ray diffraction (pXRD) is a non-destructive technique used to investigate materials' crystallinity and crystal structure. The method relies on the diffraction of monochromatic X-ray beams on a crystalline lattice. Cathode ray tube (commonly Cu, Co or Mo) generates the X-rays. The X-ray beam is focused on the sample and diffracts upon the interaction with the atoms present in the crystal lattice (Figure 2). However, the diffracted rays interfere constructively only at certain angles where the diffraction peaks can be observed. The respective angles between the incident and diffracted beam, 2θ , correlate to spacing between atoms in the grid, d , according to Bragg's law:

$$n\lambda = 2d \sin \theta$$

in which n is integer and λ is wavelength of X-ray beam (e.g. $\lambda(\text{Cu-K}\alpha) \approx 1.54 \text{ \AA}$).

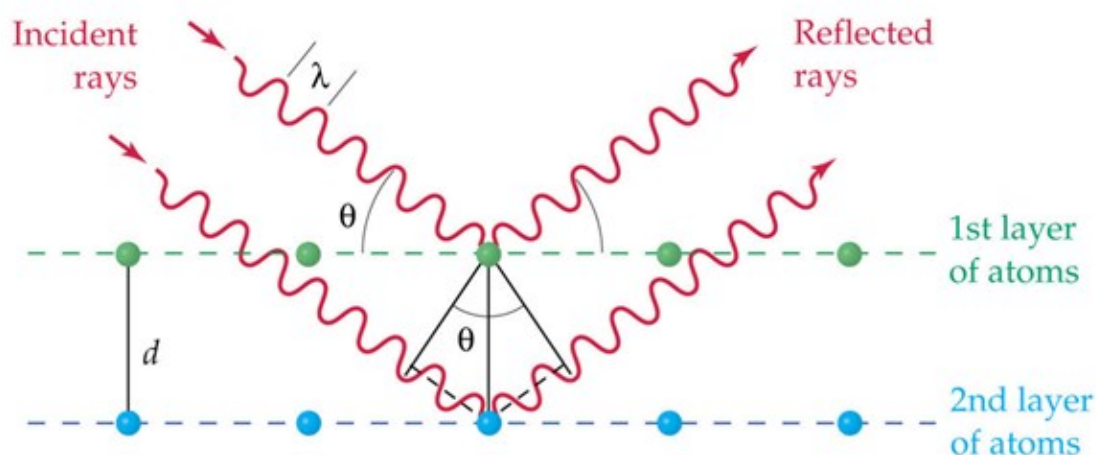


Figure 2: Bragg's law scheme ⁴⁴

The diffraction pattern provides information about crystal structure and phase purity. Upon deeper analysis we can solve the crystal structure, or determine grain size and presence of crystal defects. However, diffraction patterns can also be considered as a fingerprint of specific crystal structure; and therefore, used for phase identification by comparing the experimental diffraction pattern to a database (e.g. IZA database of zeolite structures). ^{45, 46}

N₂ adsorption-desorption is a method that analyses material's textural properties such as external surface, pore size and pore volume using physisorption of nitrogen gas. The analysis results in adsorption isotherm which can be used to determine the said properties.⁴⁷ Typically, the sample is outgassed in vacuum to remove adsorbed water prior to the measurement. Removal of physisorbed water is crucial to ensure validity of the adsorption data.⁴⁸ The measurement is performed at the temperature $-195.85\text{ }^{\circ}\text{C}$ (boiling temperature of nitrogen). During the measurement, the sample is dosed with defined volumes of nitrogen, which then adsorbs on the material. First, at low pressure nitrogen adsorbs to energetically more favourable places, such as pores. With increasing pressure, nitrogen occupies also places that are less energetically favourable. We increase the pressure up to the saturation pressure (when condensation of adsorbed molecules begins) and afterwards we decrease the pressure in a stepwise manner. A hysteresis loop on the adsorption isotherm may occur if the sample contains mesopores. This is caused by different mechanism of gas occupying and leaving the mesopores. Adsorption isotherms show dependence of volume of absorbed nitrogen on relative pressure. According to IUPAC classification, we distinguish between 6 types of isotherm shapes (Figure 3). Each type represents the shape of the isotherm typical for e.g. presence of micropores or mesopores, by weak/strong adsorbent-adsorbate interactions or multilayer adsorption.⁴⁹

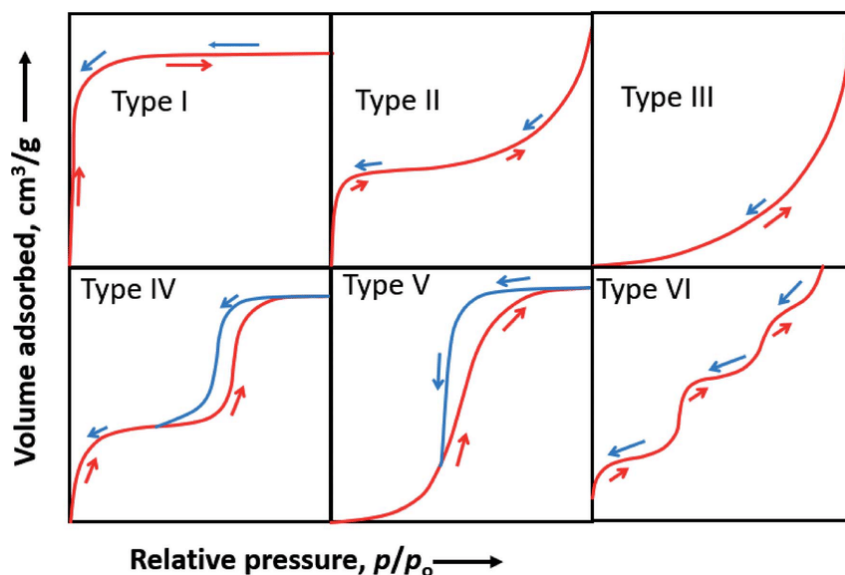


Figure 3: Different types of adsorption isotherms: Type I = Micropores; Type II = Micro mesoporous; Type III = Weak interaction; Type IV = Mesopores + capillary condensation; Type V = Weak interaction; Type VI = Layering⁵⁰

The surface area of the sample is calculated from adsorption isotherm BET (Brunauer-Emmett-Teller) method. BET method is an extension to the Langmuir theory: the surface contains equivalent adsorption sites, occupation of the sites does not influence the energy of neighbouring sites. In case of BET, first layer of adsorbed molecules acts as sites for further adsorption which gradually leads to the creation of a multilayer. ^{51, 52}

First, monolayer capacity, v_m , is to be calculated from the best linear fit of the isotherm. The surface area, S_{total} , is then calculated from the monolayer capacity according to equation:

$$S_{total} = \frac{v_m \cdot N_A \cdot S_{N_2}}{V_{N_2}}$$

in which N_A is Avogadro's number, S_{N_2} is the cross sectional area of the adsorbate, which in case of nitrogen molecule equals 0.162 nm² and V_{N_2} is the molar volume of adsorbed nitrogen that equals 22,414 dm³.

Specific surface area, S_{spec} , is calculated according to equation:

$$S_{spec} = \frac{S_{total}}{m_A}$$

in which surface area, S_{total} , is divided by the mass of adsorbent, m_A . Specific surface is often used to compare the surface of different materials such as catalysts. ^{48, 51, 52}

Fourier-transform infrared spectroscopy (FTIR) can detect changes in vibrational states of molecules. Only vibrations in which the dipole moment changes are visible by the infrared spectroscopy. The energy of the bands corresponds to the difference between lower and higher vibrational states of a certain bond. The wavelength corresponds to the strength of detected bond and intensity of obtained signal corresponds to concentration of these bonds present in the sample. Certain wavelengths are also characteristic for specific functional groups and thus can be used for their identification.

The zeolite framework contains large amounts of similar Si-O bonds making determination of the structure from FTIR problematic. However, the method can be coupled with chemisorption of basic molecules onto the zeolite to probe its concentration of acid sites. First, the probe molecules (e.g. pyridine, acetonitrile, ammonia, di-tert-butylpyridine) adsorb onto the zeolite. Interaction of the base with the acid site alters its vibration frequency (in case of pyridine – combined stretching and in-plane C–H and/or N–H bending vibrations of pyridine⁵³) making it possible to distinguish different types of acid sites (Brønsted, Lewis). Subsequently, increasing the temperature leads to a partial or complete desorption of basic molecules adsorbed to acid sites in the structure, giving us information about the relative strength of diverse acid sites. Vibrations of pyridine rings interacting with Brønsted and Lewis acid sites are observable at 1545 cm^{-1} and 1450 cm^{-1} , respectively (Figure 4).^{31, 54}

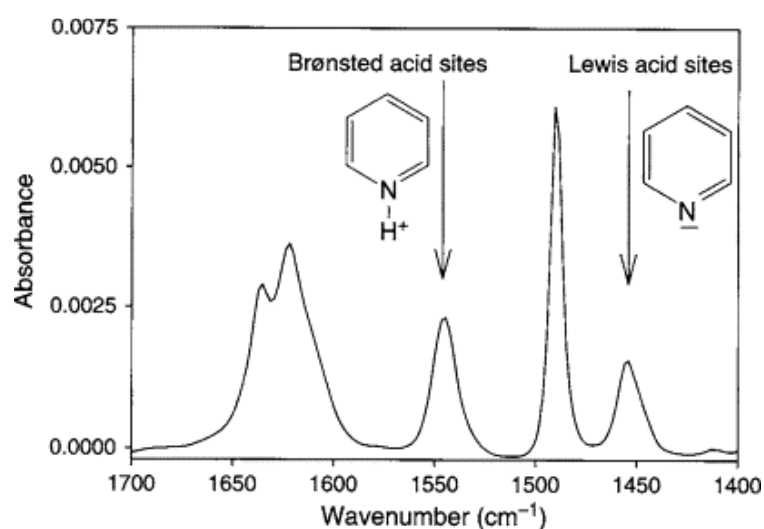


Figure 4: FTIR spectra – vibrations of pyridine rings adsorbed on Brønsted (1545 cm^{-1}) and Lewis acid sites (1450 cm^{-1})⁵⁵

3.2 Catalysis

Catalysis is a process that accelerates chemical reactions to reach equilibrium using a catalyst. Catalyst is a chemical compound or material, which lowers activation energy by changing the mechanism of the catalysed reaction, while the structure, composition and amount of catalyst entering and exiting the chemical reaction remain unchanged. About 90% of industrial chemical processes involve catalysts at least in one step of the reaction.²⁶

3.2.1 Homogeneous and heterogeneous catalysis

In homogeneous catalysis both reactants (and products) and catalyst are in the same phase. Catalysts are typically small molecules (e.g. AlCl_3 , PdCl_2 , Ziegler-Natta catalyst) dissolved in solvent, meaning diffusion does not affect the rate of the reaction. Moreover, all active centres are available for the reactants and the potential of the catalyst is thus fully utilised. However, the main disadvantage of homogeneous catalysts is their challenging separation from reaction mixtures. The need to separate the catalyst is essential especially in large industrial processes - because the presence of the catalyst impairs the purity of the product and in some cases longer presence of the catalyst in the reaction mixture can even promote undesired follow-up reactions.

On the other hand, in heterogeneous catalysis, the catalyst is in a different phase than reactants. Most commonly, the catalyst is a solid while reactants are in a gaseous or liquid form. This makes separation of the catalyst and recovery of the products significantly easier. Catalyst can be simply centrifuged or filtered off the reaction mixture. In addition, separated catalyst could be then regenerated and reused several times making it more cost efficient. For these reasons, heterogeneous catalysts are used in the majority of industrial processes. However, the disadvantages of heterogeneous catalysis include limited diffusion of reactants/products to/from the catalyst surface and limited usage of the bulk volume of the active phase. The reaction commonly proceeds over accessible centres on the catalyst surface or also inside the pores of catalyst as in the case of zeolites. Important heterogeneously catalysed processes include fluid catalytic cracking of oil, hydrocracking, and isomerisation of hydrocarbons to obtain better quality fuels.²⁶

3.2.2 Mechanisms and principles

Regardless of the exact reaction mechanism, the heterogeneous catalytic reaction always consists of 7 steps: external reactant diffusion, internal reactant diffusion, reactant adsorption, chemical reaction, product desorption, internal product diffusion and external product diffusion.

The reaction proceeds in either diffusion or kinetic mode, depending on whether the diffusion or chemical reaction is the rate determining step. In the diffusion mode, reaction rate depends mainly on the rate of external or internal diffusion. As a result, the catalyst is not used to its full potential. Slow external diffusion can be tackled for example by faster stirring of the reaction mixture. The internal diffusion can be enhanced by increasing the external surface of the catalyst ⁵⁶, for example by reducing its particle size. In the case of kinetic mode, the rate determining step is adsorption of reactants, catalytic reaction or desorption of products.

Optimisation of the reaction rate involves balancing out the strength of adsorption of reactants and products to the catalyst (Sabatier principle). If one of these interactions is significantly stronger the reaction is inhibited. This is described by the Volcano plot, which represents the dependence of the reaction rate on the strength of adsorption of reactants and products. The strength of adsorption can be optimised by carefully choosing a catalyst with the proper type of active sites. ^{57, 58}

3.2.3 Evaluation of the catalytic experiment

There are countless methods to evaluate results of catalytic experiments. In this thesis, gas chromatography was used due to the nature of the reaction mixture, which contains stable components with relatively low boiling points (up to 244 °C in the case of product, N-methylformanilide). This method is capable of determining the concentration of individual components of the reaction mixture. Knowing the concentrations enables calculation of conversion of reactants, observation of product formation and learning about selectivity of reaction.

The principle of gas chromatography is based on different strengths of adsorption of components in reaction mixture to a stationary phase. Gas chromatograph contains a column placed in the oven, through which vaporised samples travel towards the detector (Figure 5). Samples are transferred by mobile phase, unreactive carrier gas (such as nitrogen, helium or argon) under continuous flow. Samples are not separated only based on their different boiling points, but they are also further delayed by interaction with the stationary phase inside the column depending on their other properties such as size or polarity.

Samples separated in the column reach a detector, each at a different time, called retention time (molecules with low boiling temperature or weak interaction with the active phase of the column have shorter retention times). The compounds are detected by detectors, such as FID (flame ionisation detector), TCD (thermal conductivity detector) or MS (mass spectrometer).

The areas of the chromatographic peaks correlate with molar amounts of detected compounds. To evaluate changes in concentrations of reactant or products in time, an internal standard is added to the reaction mixture. Internal standard is a compound that does not interact with the reaction mixture in any way and its concentration therefore remains unchanged during the reaction and thus serves as a reference.⁵⁹

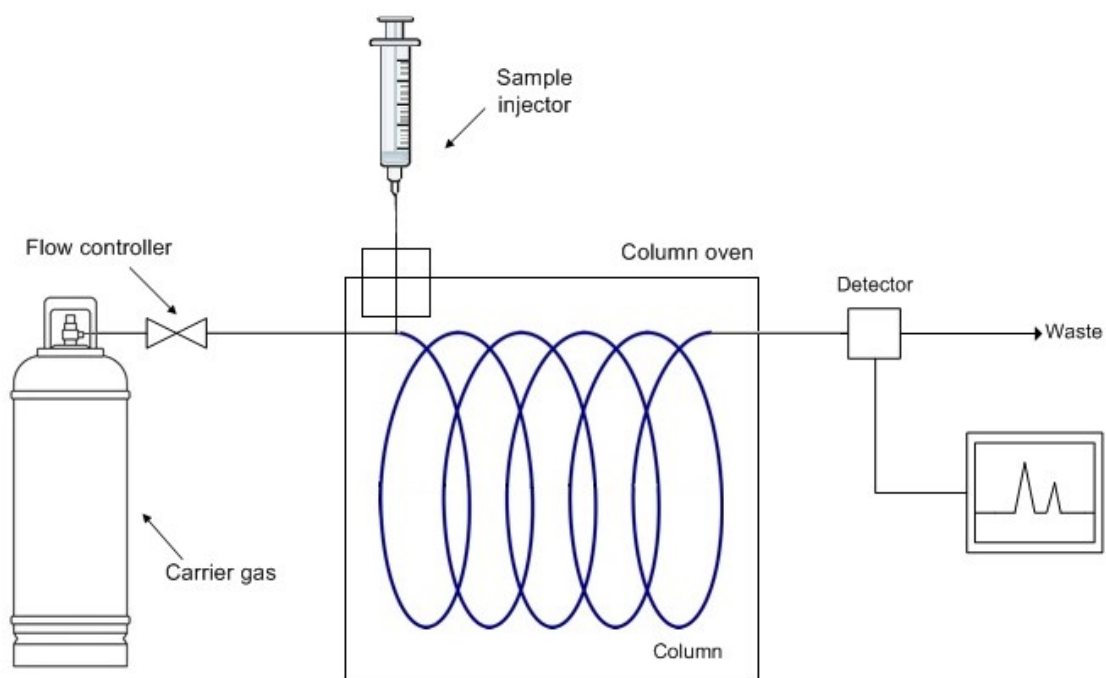


Figure 5: Diagram of a gas chromatography apparatus

3.2.4 Zeolites in catalysis

The range of applications of zeolites spans from water purification to catalysis. 70 % of produced zeolites are used as water softeners in detergents thanks to their ion-exchange ability. About 20 % are used as heterogeneous catalysts and about 10 % as adsorbents.^{60–63}

However, this thesis exclusively focuses on application of zeolites in catalysis. Zeolite's benefits include their high acidity, shape-selectivity as well as their low cost, easy regeneration and thermal stability. The most important processes catalysed by zeolites include fluid catalytic cracking (FCC) of oil, hydro-cracking (HDC) or biomass conversion.^{63–69}

Fluid catalytic cracking is the process of decreasing molecular size of heavy oil fractions to lighter fractions including gasoline, diesel or ethylene/propylene (for synthesis of polymers). The benefit of zeolites lies in their ability to catalyse formation of these products more selectively.^{63, 64, 65}

Other important processes are hydrocracking of heavy petroleum distillates (resulting in a higher yield of gasoline fraction and lower yield of coke), octane number enhancement, the synthesis of ethylbenzene or disproportionation of toluene to benzene and xylenes (xylenes are later used as precursors of terephthalic acid).^{61, 70}

Last but not least, zeolites participate in the current efforts to find renewable fuels by valorisation of biomass components. The valorisation typically involves cracking or pyrolysis of complex organic molecules in an anaerobic environment to decompose into smaller fragments such as, gaseous CO, CO₂ or light hydrocarbons. The main benefit of zeolites in catalytic pyrolysis is their ability to limit coke formation and thereby increase the yield of aromatics such as benzene, toluene, xylene and naphthalene. From the novel biomass conversion, it is also worth mentioning isomerisation of glucose to fructose (over e.g. Sn-Beta), the epimerization of sugars (e.g. Ti-Beta) or the conversion of sugars to lactic acid derivatives over zeolites, (e.g. Hf-, Zr- and Sn-Beta, Sn-MFI, Sn-MWW).^{68, 69, 71}

Zeolites are also used as catalysts in syntheses of fine chemicals (fragrances, cosmetics and also as intermediates for synthesis of drugs or dyes) due to their shape selectivity. Examples of reactions catalysed by zeolites include double-bond isomerisations, oxidations of alcohols to aldehydes or ketones, or aldol condensation reactions.^{69, 72–74}

3.3 Formylation

Formylation is a chemical reaction, in which formamides form by reaction of amines with formylating reagents (e.g. HCOOH , CO_2). Formamides contain a $\text{C}=\text{O}$ bond that is directly adjacent to the nitrogen atom. They have significant importance in organic synthesis as intermediates in synthesis of fungicides⁷⁵ and pharmaceuticals (e.g. quinolone antibiotics⁷⁶ or potential cancerocidal agents⁷⁷). Formamides are also used as reagents in Vilsmeier formylation reaction² or as catalysts in allylation and hydrosilation of carbonyl compounds.⁴

3.3.1 Mechanism

Several articles describe the impact of Lewis acid catalysts on formylation of various amines, using formic acid. In the study of *Chandra Shekhar* et al., the best yields were obtained using ZnCl_2 , SnCl_2 and LaCl_3 (>90%), or FeCl_3 , AlCl_3 , and NiCl_2 (80–90%). Further formylation reactions catalysed by ZnCl_2 showed that arylamines with electron-donating groups tend to be more active in contrast to the amines substituted with electron-withdrawing groups.⁷⁸

Reaction mechanism shown in Figure 6 was proposed. The Lewis acid catalyst withdraws electron density from the carbonyl group of formic acid. The acid then undergoes nucleophilic attack by amine, which correlates with a greater reactivity of arylamines with electron-donating groups. Lastly, water molecule is eliminated to yield the formylated product.

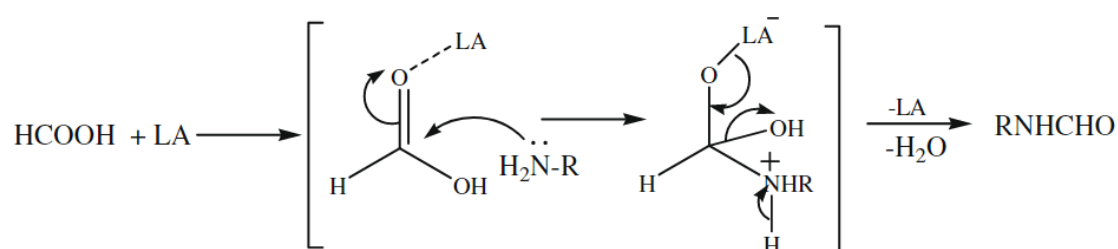


Figure 6: Mechanism of Lewis acid-catalysed N-formylation of amines with formic acid⁷⁸

3.3.2 Formylation over zeolites

Literature also provides several examples of formylation catalysed by both H^+ and ion exchanged zeolites.

Formylation of aniline with glycolic acid and H_2O_2 in 1,4-dioxane, at 70 °C, led in 12 hours to 99% yields, when Cu-containing zeolite 5A (Cu/5A) was used as catalyst, 25% in case of Cu/MCM-41 and 17% in case of Cu/HY.⁷⁹

Different articles reported that uncatalysed formylation of 4-chloroaniline with formic acid, under solvent-free conditions, at room temperature provided 25% yield after 100 minutes. However, the yield increased to 95% after only 15 minutes when zeolite A in either H^+ , K^+ or Mg^{2+} form was used as a catalyst.⁸⁰

According to another study, formylation of aniline with formic acid under solvent-free conditions at room temperature over natrolite zeolite provided up to 96 % yields in 17 minutes. Moreover, the catalyst could be also re-used up to 5 times with no observable decrease in its activity. In contrast, the reaction in the absence of a catalyst did not proceed at all even after 5 hours. According to FE-SEM and TEM pictures, copper nanoparticles were observed on crystal surface, which brings the question whether they may be responsible for the catalytic activity.⁸¹

Last but not least, formylation of aniline over nanosized CuO/HZSM-5 catalyst prepared by wet impregnation was reported. The reaction under solvent-free conditions, at room temperature, provided 97% yield in 15 minutes in contrast to other catalysts such as natrolite zeolite or HZSM-5 with 87% and 89% yields, respectively. The reaction in the absence of a catalyst at room temperature yielded no product even after 4 hours.⁸²

On one hand, these studies demonstrate that zeolites could potentially be used for catalysis of formylation. On the other hand, they do not provide clear explanation on which active sites or properties of the catalyst determine the catalytic activity. Therefore, the main subject of this thesis is to verify, whether zeolites can catalyse the formylation of amines and explain what type of active sites are the most suitable for the catalysis.

4 Experimental Part

4.1 List of used chemicals

Table 1: List of used chemicals

Chemical	Formula/Abbreviation	Purity	Manufacturer
Aluminium nitrate nonahydrate	$\text{Al}(\text{NO}_3)_3 \cdot 9 \text{H}_2\text{O}$	$\geq 98\%$	Sigma Aldrich
Ammonium nitrate	NH_4NO_3	$\geq 99\%$	Sigma Aldrich
Copper (II) acetate	$\text{Cu}(\text{CH}_3\text{COO})_2$	98%	Sigma Aldrich
Dimethylformamide	DMF	$\geq 98\%$	VWR Chemicals
1,4-Dioxan	DIO	$\geq 99\%$	VWR Chemicals
Formic acid	HCOOH	$\geq 95\%$	Sigma Aldrich
Hydrochloric acid	HCl	37%	Sigma Aldrich
Mesitylene	-	98%	Alfa Aesar
Methanol	MeOH	P.A.	LACHNER
N-methylaniline	-	98%	Sigma Aldrich
Silicon dioxide	SiO_2 /Fumed silica	99,5%	Sigma Aldrich
Tetraethylammonium hydroxide	TEAOH	35%	Thermo Scientific

4.2 Synthesis of Beta zeolites

Aluminosilicate Beta zeolite was synthesised using the hydrothermal synthesis method described in ⁸³. First, 67.50 g of 35% TEAOH was diluted with 57.22 ml of distilled water. Subsequently, 5.24 g of 37% HCl and 6.64 g of $\text{Al}(\text{NO}_3)_3 \cdot 9 \text{H}_2\text{O}$ was added to the mixture. The mixture was stirred for 30 minutes and subsequently added to a beaker with 16.00 g of fumed silica under constant stirring. The final gel molar composition was:



The mixture was poured into 90ml Teflon-lined steel autoclaves. The crystallisation was carried out under static conditions and temperature 140 °C for 14 days. The autoclaves were cooled rapidly and solid products recovered by centrifugation at 4500 rpm for 10 minutes. The zeolite was dried overnight at 60°C and calcined in a flow of air at 560 °C for 8 hours.

The obtained Beta zeolite was exchanged into NH_4^+ form using 1M solution of NH_4NO_3 in ratio 1 g of sample in 100 ml of solution. The mixture was stirred for 4 hours at room temperature. After that, sample was centrifuged and the aqueous solution replaced with fresh 1M NH_4NO_3 . This process was repeated 4 times. Sample in NH_4^+ form was calcined on air at 550 °C for 8 hours to obtain the H^+ form.

The ion exchange of the H^+ Beta into Cu^{2+} form was carried out in into 0.1M solution of $\text{Cu}(\text{CH}_3\text{COO})_2$ in ratio 1 g of sample in 100 ml of solution and stirred overnight. The sample was recovered by centrifugation, washed with distilled water and dried at 60°C. Lastly, the dry sample was then calcined at 550 °C for 8 hours.

Stannosilicate Beta zeolite was synthesised using the hydrothermal synthesis method. First, 35.17 g of tetraorthosilicate (TEOS) was dissolved in 37.59 g of 35% TEAOH. In another beaker, 0.58 g of SnCl_4 was dissolved in 1.5 ml of distilled water and added dropwise into the first mixture. The mixture was stirred at 100 °C to allow hydrolysis of the TEOS and complete evaporation of produced ethanol. Subsequently, 1.00 of pure-Si zeolite Beta seeds were added into the mixture. After their dissolution, 3.73 g of 48% HF was added. The resulting mixture was transferred to a 90 ml Teflon-lined stainless steel autoclave. The crystallisation was carried out under static conditions and temperature 140 °C for 18 days. The autoclaves were cooled rapidly and solid products were recovered by filtration. The zeolite was dried overnight at 60°C and calcined in a flow of air at 550 °C for 6 hours.

4.3 Characterisation of Beta zeolites

The **crystal structure** of prepared zeolites was verified using powder XRD diffraction. The measurement was performed using a Bruker D8 Advance diffractometer equipped with a Linxeye XE-T detector in the Bragg–Brentano geometry using Cu $\text{K}\alpha$ radiation with wavelength 0.15406 nm. Zeolite (powder) was pressed into a plastic holder. Each sample was measured in 3-40° 2θ range with 0.021° step size and 0.8 s time per step. Obtained diffraction patterns were compared with literature.²²

Textural properties of prepared zeolites were determined from nitrogen adsorption isotherms. The measurement was performed using Micromeritics 3Flex volumetric surface area analyser. First, samples were degassed using Micromeritics Smart Vac Prep instrument, which utilises vacuum to prepare samples by heating at 250 °C for 8 hours with heating rate 1 °C min⁻¹ and evacuation to 3.10⁻² mmHg. Next, the nitrogen adsorption/desorption was performed. The BET area was determined from obtained adsorption isotherms (dependences of the adsorbed volume of nitrogen on the relative pressure) in the relative pressure range from $p/p_0 = 0.05$ to $p/p_0 = 0.25$. The micropore volume and external surface area were obtained using the t-plot method.

To determine **concentration and type of acid sites** in prepared samples, FTIR coupled with adsorption of pyridine was used. The measurement was performed using FTIR spectrometer Thermo Nicolet 6700. First, wafers from the powdered samples were prepared using a press (force 20-30 kN), having a parameters corresponding to 8-12 mg of sample per 1 cm² of surface. Before the measurement, the wafers were activated in quartz IR cell at 450 °C with the heating rate of 5 °C/min under vacuum conditions for 4h. Next, first spectrum was measured from 4000 to 400 cm⁻¹ and after that pyridine was adsorbed at 150 °C. Physisorbed pyridine was desorbed at the same temperature of 150 °C in a vacuum. The baseline was obtained from the difference between the spectra measured after activation and the spectra obtained during the desorption measurement. The concentrations of Brønsted and Lewis acid centres were determined from obtained spectra (dependences of absorbance on the wavenumbers of IR-radiation) in the following manner: The concentration was calculated using the Lambert-Beer's law and the molar extinction coefficients of $\epsilon(B) = 1.67 \pm 0.1 \text{ cm } \mu\text{mol}^{-1}$ and $\epsilon(L) = 2.22 \pm 0.1 \text{ cm } \mu\text{mol}^{-1}$, found in the literature.⁸⁴

4.4 Catalytic experiments

First, calibration of gas chromatograph Agilent 7890B GC equipped with HP-5 column (length 30 m, diameter 0.320 mm, and film thickness 0.25 μm) and flame ionisation detector was done in the following manner: Specific amounts of reactant and product were weighed on analytical balances using syringes. Three solutions of the reactant and the product in

1,4-dioxane were prepared in such a way that each of the solutions contained different concentrations of these components. Such prepared solutions were analysed by gas chromatograph and the dependences of the detector response on the given concentration were compiled from the obtained data. In this way, the response factors for both the reactant and the product were obtained, which were further used to calculate the yield and selectivity of the reactions carried out.

Catalytic experiments were performed in 25 ml round-bottom flasks with magnetic stirrer in multi-experiment workstation Starfish™. Before the experiment, catalysts were activated in the oven at 450 °C for 6h. Then 0.1 g of catalyst was weighted and put into flask with 10 ml of solution (dioxane/dimethylformamide/methanol). The flask was placed into the Starfish, connected to reflux cooler and sealed with septum. Mesitylene was used as an internal standard. 0.1 g of mesitylene was weighted and added to the reaction mixture using syringe. Next, 0.5358 g of N-methylaniline was weighted and added to the mixture. After that, first sample was taken. The reaction was initiated by addition of 0.2762 g HCOOH. (The molar ratio of HCOOH: N-methylaniline was 6: 5). Samples were collected periodically up to 24 hours, and analysed by gas chromatograph Agilent 7890B GC equipped with HP-5 column (length 30 m, diameter 0.320 mm, and film thickness 0.25 µm) and flame ionisation detector.

Another set of catalytic experiments was performed in 50 ml round-bottom flasks with magnetic stirrer in apparatus connected to circulating thermostat Julabo (model F12), to ensure constant temperature of reaction mixture throughout the whole experiment. The experiments were performed in double the amount in order to obtain more accurate data. Samples were collected and analysed as in the previous case.

5 Results and discussion

5.1 Synthesis and characterisation of catalysts

The aluminosilicate and stannosilicate Beta zeolites were synthesised via hydrothermal crystallization. Cu/Beta was prepared via ion exchange of H⁺Beta in 0.1M solution of Cu(CH₃COO)₂. **Crystal structure** of synthesised zeolites was confirmed using powder XRD analysis. Obtained diffraction patterns (Figure 7) were compared to theoretical diffraction pattern of the Beta zeolite obtained from the IZA database.²² Characteristic reflections at 7.7, 13.8, 14.4, 21.3 and 22.3° 2θ confirm the synthesised materials possess the Beta structure.

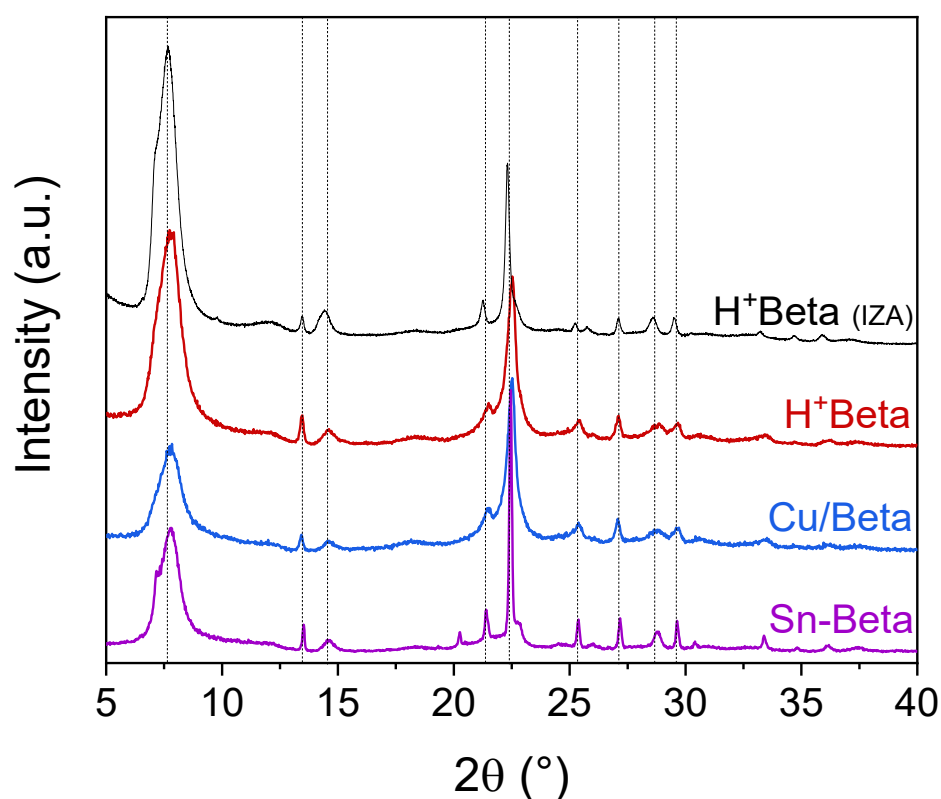


Figure 7: Powder XRD patterns of synthesised Beta zeolites and reference XRD pattern obtained from IZA database

Textural properties of the Beta zeolites, including BET area, micropore volume and external surface area, were determined from nitrogen adsorption isotherms shown in Figure 8. Sn-Beta samples exhibit Type I. isotherm according to IUPAC classification. This type is characteristic for microporous materials such as zeolites. H⁺Beta and Cu/Beta exhibit Type II. isotherm with narrow hysteresis loop which implies the presence of both micro and mesopores.

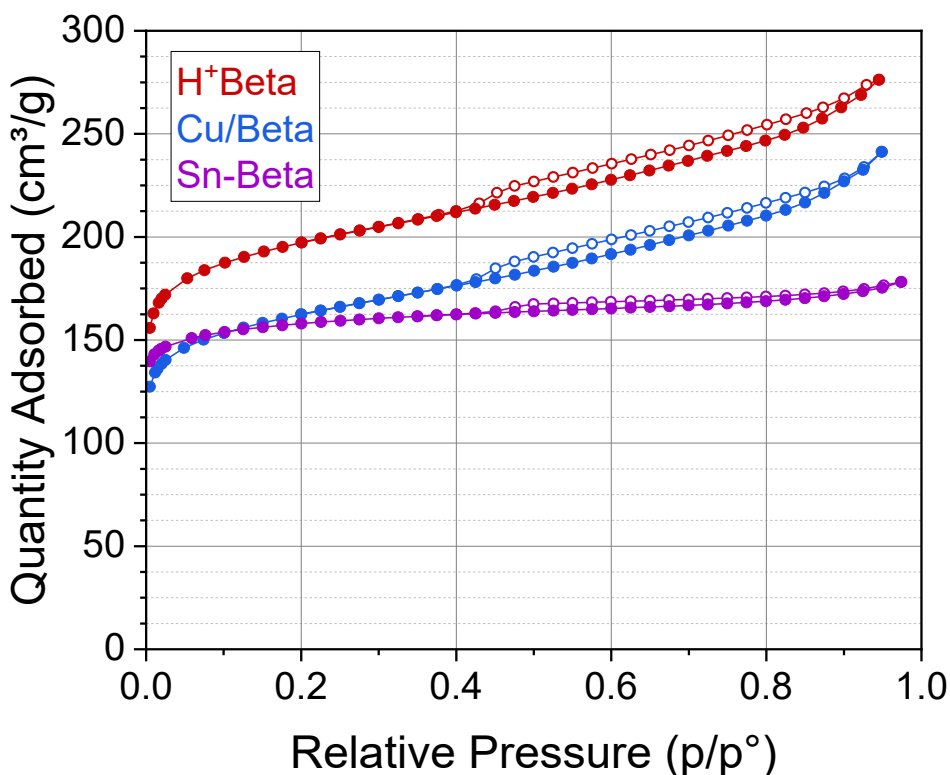


Figure 8: Nitrogen adsorption-desorption isotherms of synthesised Beta zeolites

The samples possessed BET area from 546 to 688 m²/g and micropore volumes from 0.17 to 0.22 which is typical for Beta zeolites according to the literature.²² Decrease in BET area and micropore volume in case of Cu/Beta compared to H⁺Beta is caused by larger copper ions occupying the pores. The results obtained are shown in Table 2.

Table 2: Textural properties of the Beta zeolites determined by N₂ adsorption/desorption

	BET (m ² /g)	S _{ext} (m ² /g)	V _{tot} (cm ³ /g)	V _{mic} (cm ³ /g)
H ⁺ Beta	688	206	0.43	0.22
Cu/Beta	560	190	0.37	0.17
Sn-Beta	546	80	0.28	0.21

Acidic properties of the zeolites were determined by pyridine adsorption coupled with FTIR spectroscopy. The FTIR spectra are shown in Figure 9. We can observe the vibrations of OH groups between 3800 and 3400 cm⁻¹. Peak at 3745 cm⁻¹ corresponds to vibrations of Si-OH bonds present in defects and on the external surface of the samples. Peak at 3610 cm⁻¹ corresponds to vibrations of Brønsted acidic Si-(OH)-Al bridging groups

present in the aluminosilicate Beta samples (i.e. H⁺Beta and Cu/Beta). These signals disappear after pyridine adsorption to the Brønsted sites.⁸⁴ The peak at 3680 cm⁻¹ in the spectrum of Cu/Beta corresponds to vibrations hydrated complexes of Cu²⁺ ions such as [Cu(H₂O)_n]²⁺ or [Cu(OH)(H₂O)_n]⁺.⁸⁵

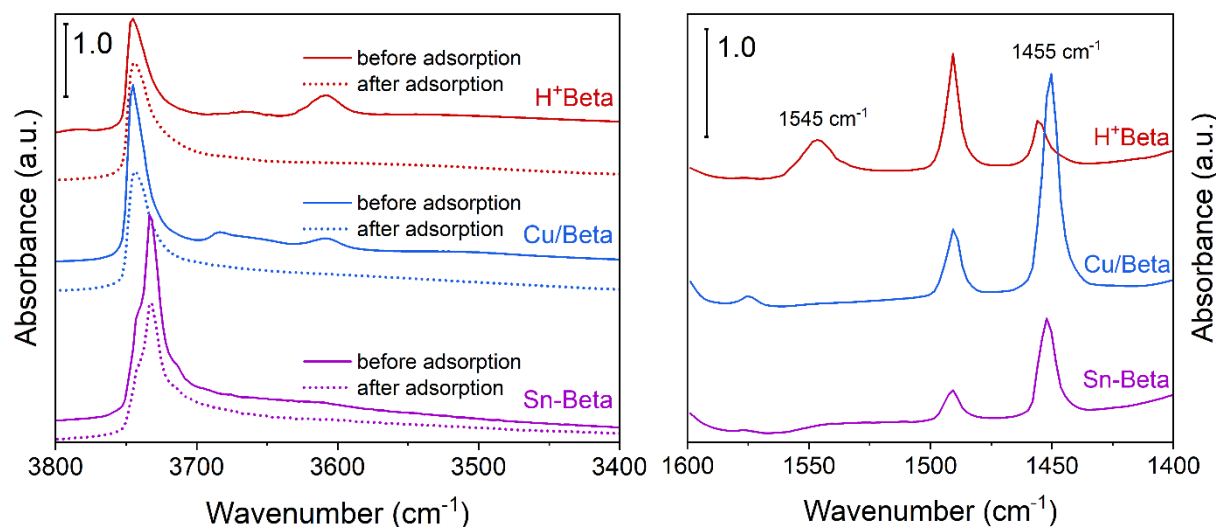


Figure 9: FTIR spectra of the OH group vibrations of the Beta zeolites (left) and of pyridine ring interacting with Brønsted (1545 cm⁻¹) and Lewis acid sites (1455 cm⁻¹) on the Beta zeolites (right).

The wavenumber region 1600–1400 cm⁻¹ shows the vibrations of the pyridine ring. We can observe distinct signals at 1545 and 1455 cm⁻¹ which correspond to pyridine interacting with Brønsted and Lewis acid sites, respectively. The H⁺BEA possessed both Brønsted and Lewis acid sites. However, after its ion exchange into the Cu²⁺ form the signal of Brønsted acid sites disappeared. In the case of Sn-Beta only Lewis acid sites were observed.

The H⁺BEA possessed both Brønsted and Lewis acid sites with concentration 0.48 mmol/g and 0.21 mmol/g, respectively. The ion exchange to Cu²⁺ form inactivated the Brønsted sites and, simultaneously, the concentration of Lewis acid sites increased to 0.67 mmol/g. The Sn-Beta possessed no Brønsted sites and concentration of its Lewis acid sites equalled to 0.39 mmol/g. The concentrations of acid sites for all samples are shown in Table 3.

Table 3: Concentrations of Brønsted and Lewis acid sites of the Beta zeolites determined by pyridine adsorption coupled with FTIR spectroscopy

	C Brønsted (mmol/g)	C Lewis (mmol/g)
H⁺Beta	0.48	0.21
Cu/Beta	0.00	0.67
Sn-Beta	0.00	0.39

5.2 Catalytic experiments

As our model reaction, we chose formylation of N-methylaniline using formic acid as formylating reagent with N-methylformanilide as a product.

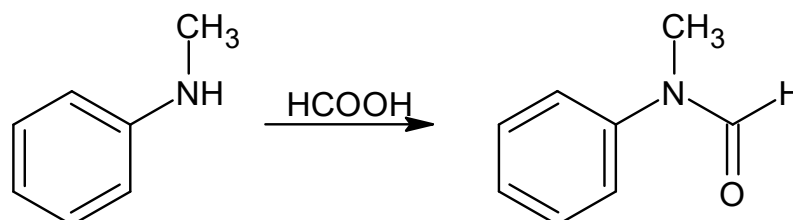


Figure 10: Scheme of formylation of N-methylaniline using formic acid with N-methylformanilide as a product

Prior to the catalytic experiments, calibrations for N-methylaniline (reactant) and N-methylformanilide (product) were performed in order to determine the relation between the concentration of each compound and the response of the flame-ionization detector. The dependency between the concentration and response is linear and its slope corresponds to its response factor. Response factors obtained for reactant and product were $f(r) = 2959.8$ and $f(p) = 3160.0$. Response factors obtained for both the reactant and the product were further used to calculate the yields of product and selectivity of the reactions. Both calibration curves are shown in Figure 11.

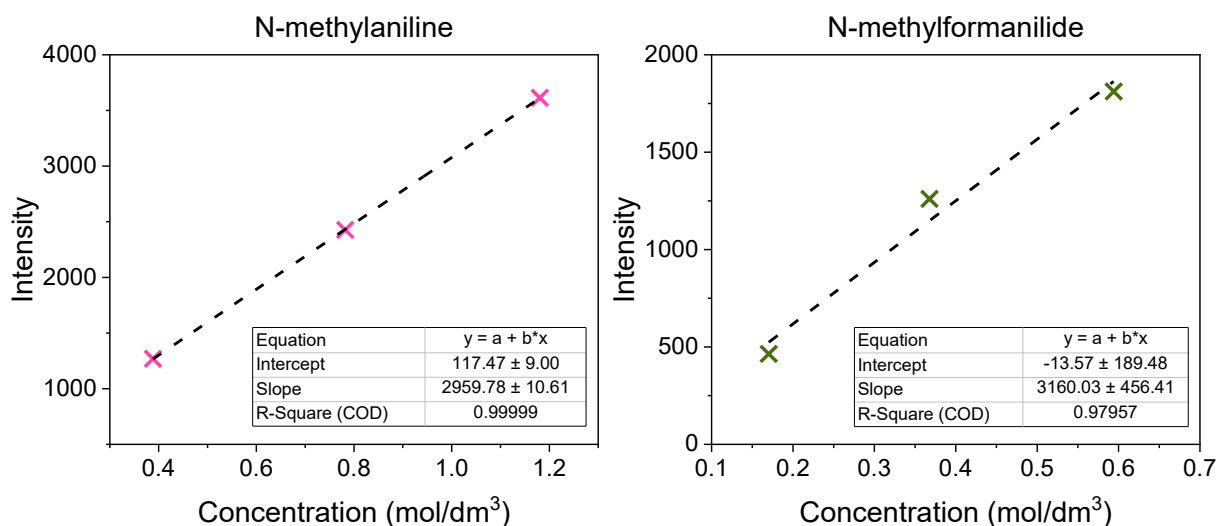


Figure 11: Calibration curves – dependence of substance concentration on detector response and corresponding response factors for N-methylaniline (reactant) and N-methylformanilide (product)

Firstly, we performed preliminary catalytic experiments to optimize the reaction conditions. We focused on choosing the most suitable solvent, concentration of reactants and reaction temperature. To select a suitable solvent, we performed separate reactions of 6 mmol of N-methylaniline in 1,4-dioxane (DIO), dimethylformamide (DMF) and mixture of DMF and methanol (DMF+MeOH) under 55 °C using Cu/Beta as a catalyst. The reaction in 1,4-dioxane (DIO) led to N-methylaniline conversion 49% after 24 hours with 46% yield (Figure 12). The mixture of dimethylformamide and methanol (DMF+MeOH) provided conversion 21% with only 7% yield and pure dimethylformamide (DMF) provided conversion only 8% with 1% yield. Hence we chose 1,4-dioxane as a solvent for the following catalytic experiments.

We also performed additional experiments under solvent-free conditions in a large excess of formic acid; however, results of the experiments were not reproducible. The high concentration of formic acid also caused additional technical problems including rapid deterioration of the catalyst and requirement to dilute the samples before analysis to avoid damaging the GC column. The dilution inherently introduced another source of inaccuracy into the results. For the above mentioned reasons, we abandoned this type of experiment.

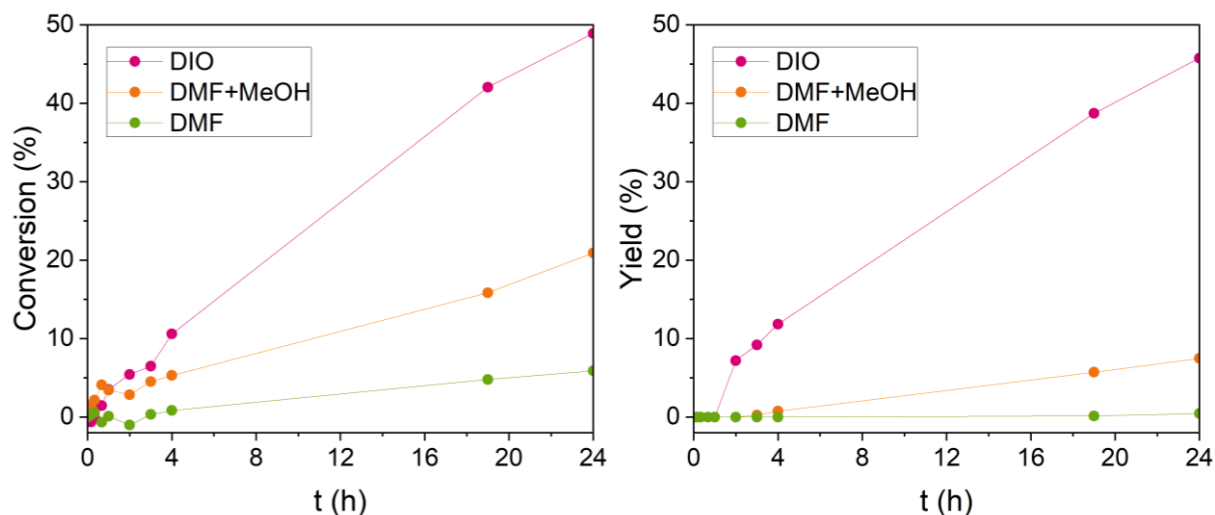


Figure 12: Conversions of N-methylaniline and yields of N-methylformanilide for reactions performed at 55 °C with Cu/Beta used as a catalyst in different solvents

We further examined the effect of concentration of both reactants on the reaction rate. We observed no reaction in a stoichiometric mixture of the two reactants. In contrast, reaction mixture with 0.5 mol/dm³ N-methylaniline with 1.2 molar excess of formic acid provided 49 % conversion after 24h (Figure 12). Therefore, all subsequent reactions were carried out in a 1.2 molar excess of formic acid. Due to the excess of HCOOH, we determined reaction conversions for N-methylaniline.

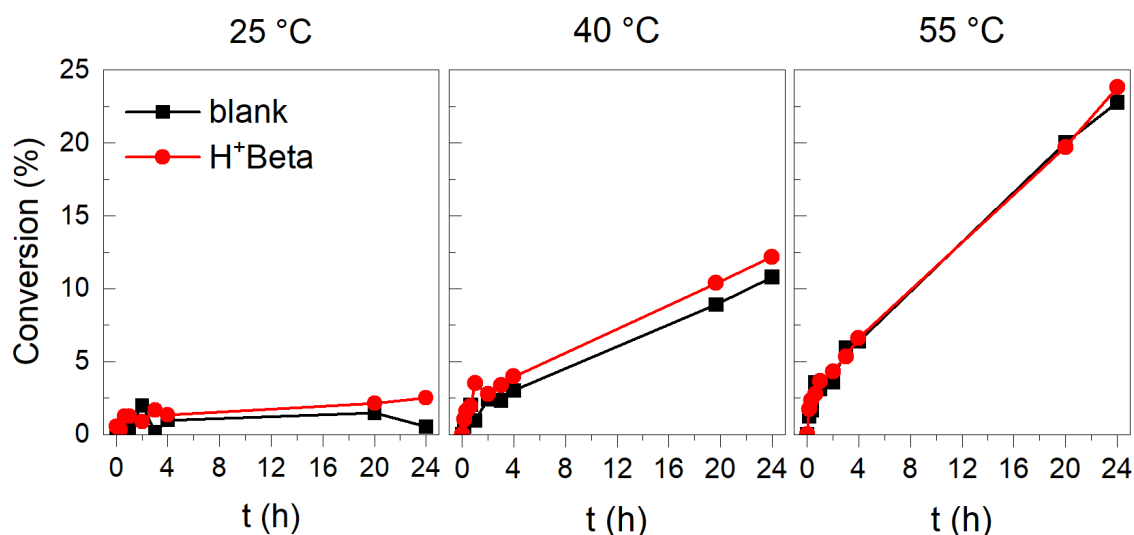


Figure 13: Conversions of spontaneous (uncatalysed) thermic reaction at different temperatures

Subsequently, we carried out a set of experiments at 25, 40 and 55 °C to determine the effect of temperature on the reaction rate. Experiments were performed both without a catalyst (“blank”) and using H⁺Beta as a catalyst. Catalyst-free reaction provided 1 % conversion under 25 °C after 24 hours. Increasing the temperature to 40 and 55 °C resulted in an increase of the conversion to 11 and 23 %, respectively (Figure 13). Experiments over the H⁺Beta did not show any significant difference from the “blank” experiments, giving 3, 12 and 24 % conversion under 25, 40 and 55 °C, respectively. Therefore, we concluded that H⁺Beta does not catalyse the reaction. However, the observations suggest that the reaction proceeds spontaneously even without the presence of a catalyst to non-negligible conversions (23 % at 55 °C) and with 96% selectivity (Figure 14).

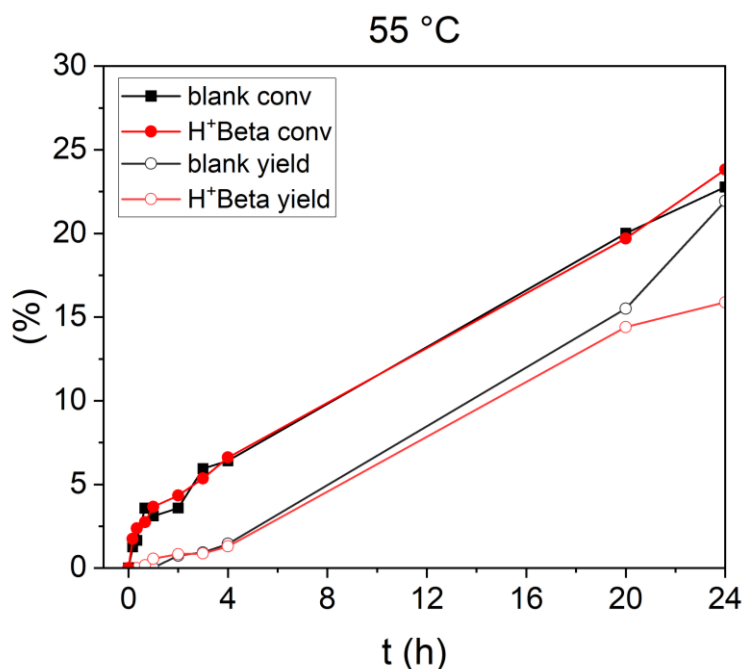


Figure 14: Conversion and yields of spontaneous (uncatalysed) thermic reaction at 55 °C

The literature (section 3.3.2) often suggests the Cu/zeolites as suitable catalysts for the formylation reaction. Therefore, we subsequently performed another set of catalytic experiments using Cu/Beta as catalyst (Figure 15). The experiments provided 4% conversion at 26 °C with 1% yield, 6% conversion at 30 °C with 2% yield, 11% conversion at 40 °C with 11% yield and 25% conversion at 55 °C with 20% yield. In contrast to the literature, the values obtained from Cu/Beta do not significantly differ from those of the “blank” experiment. This suggests that Cu/Beta does not provide any significant catalytic activity in the formylation.

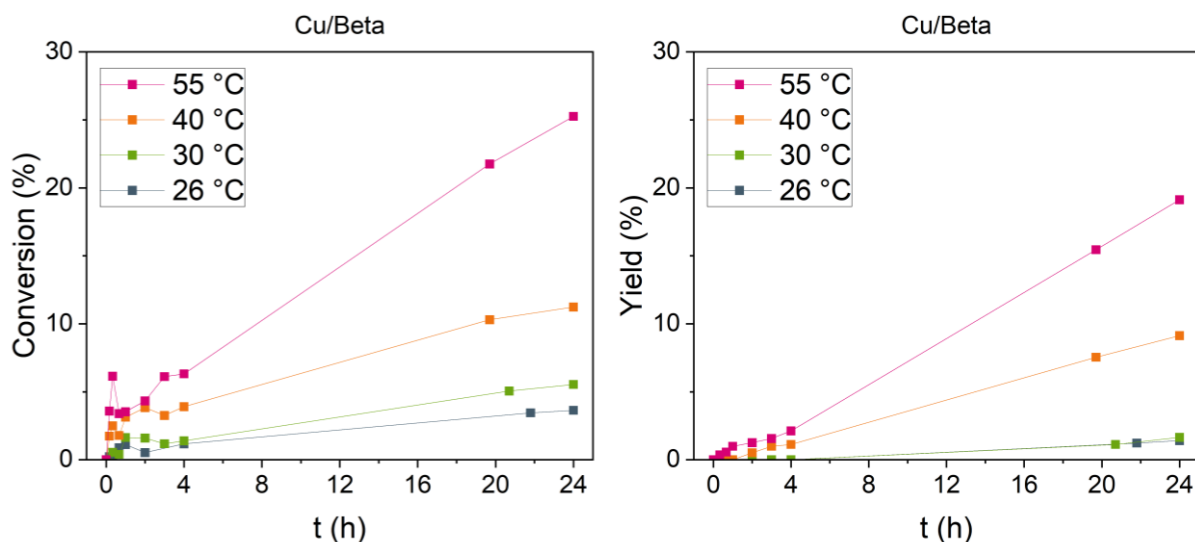


Figure 15: Conversions of N-methylaniline and yields of N-methylformanilide for reactions performed at different temperatures with Cu/Beta used as a catalyst

Furthermore, we speculated that the formic acid may leach the Cu sites from the catalyst and thus cause both its deactivation and contamination of the samples with Cu species. Our hypothesis was supported by the fact that the reaction mixture with Cu/Beta turned from yellow to green upon addition of formic acid (Figure 16). In contrast, we did not observe such colour change in the blank experiment. This alone evidences copper leaching into the solution.



Figure 16: Samples of reaction mixtures: blank (up) and with Cu/Beta catalyst (bottom), centrifuged

We performed FTIR measurement of spent Cu/Beta after the catalytic experiment to validate the theory. The spectra of fresh and spent catalyst are shown in Figure 17. We observed a decrease of concentration of Lewis acid sites (at 1455 cm^{-1}) among the two samples. Furthermore, the concentration of Brønsted acid sites (at 1545 cm^{-1}) increased. This observation can be explained by the copper being washed out of the sample resulting in the loss of Lewis acidity. Additionally, the removal of copper is accompanied by the liberation of Brønsted acid centres which were originally inactivated by the ion-exchange to the Cu^{2+} form and therefore invisible to the FTIR measurement. Simultaneously, the peak at 3680 cm^{-1} which corresponds to vibrations of hydrated Cu^{2+} species also decreased; thereby, confirming the decreased copper content.

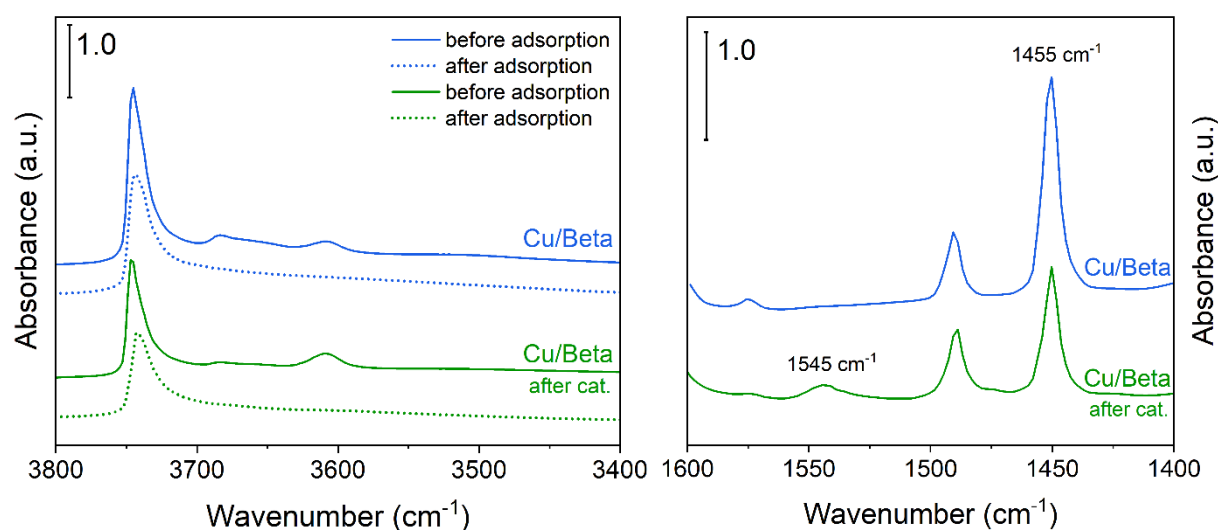


Figure 17: FTIR spectra of the OH group vibrations (left) and of pyridine ring interacting with Brønsted (1545 cm^{-1}) and Lewis acid sites (1450 cm^{-1}) (right) of Cu/Beta catalyst before and after catalysis.

The leaching of copper from Cu/Beta catalyst makes the catalyst impractical. Therefore, we decided to investigate whether it can be replaced with different Lewis acid zeolite; Sn-Beta. The Sn-Beta contains framework tin sites which are less susceptible to removal from the catalyst during the reaction compared to the copper ions.

We performed another set of catalytic tests over the Sn-Beta in a range of temperatures from 26 to 55 $^{\circ}\text{C}$ (Figure 18). The experiments provided 4% conversion at 26 $^{\circ}\text{C}$ with 1% yield, 5% conversion at 30 $^{\circ}\text{C}$ with 2% yield, 11% conversion at 40 $^{\circ}\text{C}$ with 11% yield

and 25% conversion at 55 °C with 25% yield. In other words, we observed conversions and yields very similar to both uncatalysed reaction and reaction with Cu/Beta catalyst.

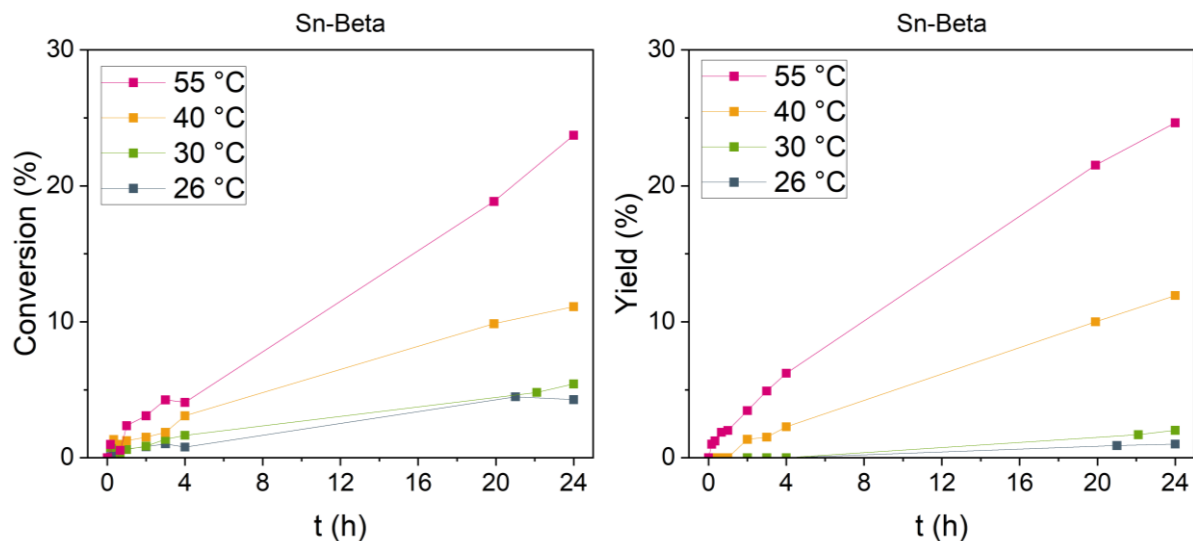


Figure 18: Conversions of N-methylaniline and yields of N-methylformanilide for reactions performed at different temperatures with Sn-Beta used as a catalyst

All described catalytic experiments were repeated several times. However, we observed a degree of inconsistency among the results from several experiments carried out under the same set of conditions (i.e. type of catalyst, solvent, reaction temperature). Since our previous experiments proved that the formylation can proceed at room temperature in the absence of a catalyst (Figure 13) we speculated that the obtained results may have been influenced by minor factors such as the delay between sample collection and analysis or ambient temperature of the laboratory. In order to minimize these factors, we repeated experiments in a thermostat set to 26 °C and analysed collected samples immediately after collection (Figure 19). The experiments provided us with reliable data. The results showed conversion 3, 3 and 4 % for the blank experiment, Cu/BEA and Sn-BEA, respectively, thus proving that neither Cu/Beta nor Sn-Beta provide any significant catalytic activity.

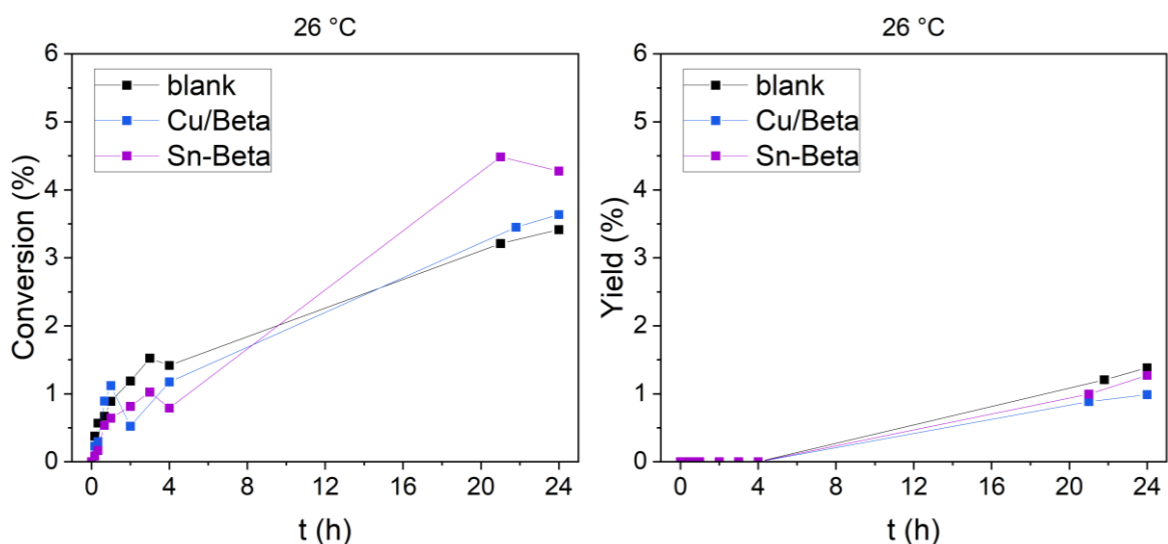


Figure 19: Conversions of N-methylaniline and yields of N-methylformanilide for reactions performed at 26 °C with different catalysts

Last but not least, we verified that the reaction proceeds in the collected samples even after removal of the catalyst. We placed the samples shown in Figure 19 into an oven heated to 50 °C for 24 hours and subsequently repeated the analysis. Results displayed in Figure 20 show that the conversion of N-methylaniline increased by almost 20 %. This experiment confirmed that the reaction continued in the samples even after they had been taken from the reaction mixture and that careful planning is essential in order to obtain valid data for the formylation experiments.

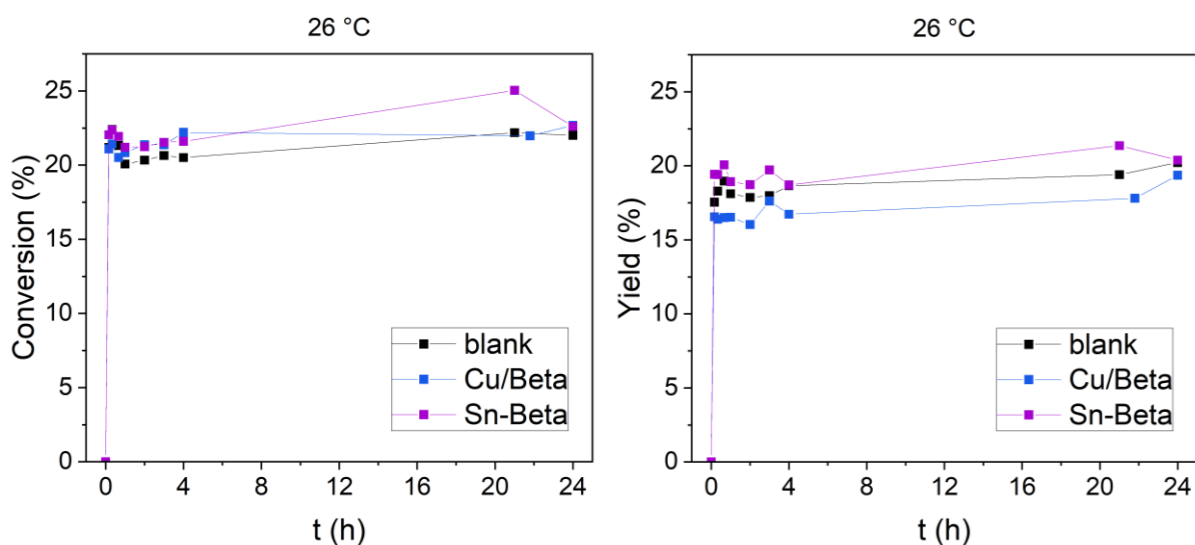


Figure 20: Conversions of N-methylaniline and yields of N-methylformanilide for reactions performed at 26 °C with different catalysts after 24 hours in oven at 50 °C

6 Conclusion

In this thesis, we aimed to clarify conflicting literature reports on formylation of amines using formic acid as a reagent over zeolite catalysts. We successfully prepared aluminosilicate Beta zeolites in H^+ and Cu^{2+} form, and also stannosilicate Beta zeolite. We characterised their properties including crystal structure, BET area, micropore volume and concentration of acid sites with powder XRD, nitrogen sorption and pyridine adsorption coupled with FTIR spectroscopy, respectively. The synthesis provided zeolite catalysts with Beta structure and textural properties comparable to materials previously published in literature.

We determined that the zeolite Beta in Cu^{2+} form (Cu/Beta) possesses primarily Lewis acid sites. This suggests that Lewis acid sites play a crucial role in the catalysis of formylation in the published literature.

We chose formylation of N-methylaniline as our model reaction. Primary tests showed that 1,4-dioxane is the most suitable solvent for the reaction. We proved that the formylation of N-methylaniline with formic acid in 1,4-dioxane proceeds even in the absence of a catalyst under mild conditions. Reaction at 55 °C provided 23 % conversion of N-methylaniline after 24 hours with 96 % selectivity. Considering that the reaction proceeds spontaneously under relatively mild conditions, we speculated whether the use of a catalyst would provide clear-cut benefits.

Initially, we chose stoichiometric concentration of both reactants, but the reaction did not proceed under such conditions. Increasing the concentration of HCOOH to 1.2 or 2 molar excess resulted in conversion of the N-methylaniline to N-methylformanilide. However, our goal was to reduce the amount of harsh chemicals (e.g. HCOOH) and also we were concerned about copper leaching; therefore, we chose lower 1.2 molar excess.

We performed a series of catalytic tests of N-methylaniline formylation over Brønsted-Lewis acid H^+ Beta and purely Lewis acid Cu/Beta and Sn-Beta in range of temperatures from 26 to 55 °C and compared the result to a catalyst-free reaction. In contrast to the published literature, we did not observe any significant difference between reactions carried out with and without any of the investigated catalysts.

In addition, we have clearly demonstrated that the presence of formic acid leads to leaching of copper from Cu/Beta zeolite into the reaction mixture, which leads not only to a decrease in its Lewis acidity, but above all in undesired contamination of the reaction mixture. This phenomenon has not been discussed in the literature. Due to the mentioned disadvantages of this catalyst, we also examined another typical Lewis catalyst – stannosilicate Beta zeolite (Sn-Beta). We have shown that Sn-Beta is more resistant to leaching compared to Cu/Beta.

Last but not least, we discovered that minor factors including ambient temperature or delay between sample collection and analysis may negatively impact the results from the experiments. Taking these effects into consideration, we repeated the experiments with additional precautions and verified that the above mentioned zeolites do not catalyse the reaction. Nevertheless, we feel a need to express concern whether the authors of the original studies have taken these details into consideration. Our results undeniably show that the reaction is sensitive to factors such as ambient temperature which makes the validity of the published results questionable.

7 References

1. Pettit, G. R. *et al.* Isolation and structures of axistatins 1-3 from the Republic of Palau marine sponge *Agelas axifera* Hentschel. *J Nat Prod* **76**, 420–424 (2013).
2. Downie, I. M., Earle, M. J., Heaney, H. & Shuhaibar, K. F. Vilsmeier formylation and glyoxylation reactions of nucleophilic aromatic compounds using pyrophosphoryl chloride. *Tetrahedron* **49**, 4015–4034 (1993).
3. Ganapati Reddy, P., Kishore Kumar, G. D. & Baskaran, S. A convenient method for the N-formylation of secondary amines and anilines using ammonium formate. *Tetrahedron Lett* **41**, 9149–9151 (2000).
4. Gerack, C. J. & McElwee-White, L. Formylation of Amines. *Molecules* **19**, 7689–7713 (2014).
5. Blicke, F. F. & Lu, C. J. Formylation of Amines with Chloral and Reduction of the N-Formyl Derivatives with Lithium Aluminum Hydride. *J Am Chem Soc* **74**, 3933–3934 (1952).
6. Vural Gursel, I., Noël, T., Wang, Q. & Hessel, V. Separation/Recycling Methods of Homogeneous Transition Metal Catalysts in Continuous Flow. *Green Chemistry* **17**, 2012–2026 (2015).
7. Barrer, R. M. Zeolites and their synthesis. **1**, 130–140 (1981).
8. Corma, A. State of the art and future challenges of zeolites as catalysts. *J Catal* **216**, 298–312 (2003).
9. Weitkamp, J. Zeolites and catalysis. *Solid State Ion* **131**, 175–188 (2000).
10. Yilmaz Ulrich Müller, B. A. Catalytic Applications of Zeolites in Chemical Industry. *Springer* **52**, 888–895 (2009).
11. Fruijtier-Pöllöth, C. The safety of synthetic zeolites used in detergents. *Arch Toxicol* **83**, 23–35 (2009).
12. Čejka Jiří, Morris Russell E. & Nachtigall Petr. *Zeolites in Catalysis: Properties and Applications*. Royal Society of Chemistry (2017).

13. Cundy, C. S. & Cox, P. A. The hydrothermal synthesis of zeolites: History and development from the earliest days to the present time. *Chem Rev* **103**, 663–701 (2003).
14. Barrer, R. M., Baynham, J. W., Bultitude, F. W. & Bleier, W. M. Hydrothermal Chemistry of Silicates. Part X1V.I Zeolite Crystallisation in Presence of Mixed Bases. *J. Chem. SOC* 983 (1970).
15. Perez-Pariente, J., A. Martens, J. & A. Jacobs, P. Crystallization mechanism of zeolite beta from (TEA)₂O, Na₂O and K₂O containing aluminosilicate gels. *Appl Catal* **31**, 35–64 (1987).
16. Sanhoob, M. A., Khan, A. & Ummer, A. C. ZSM-5 Catalysts for MTO: Effect and Optimization of the Tetrapropylammonium Hydroxide Concentration on Synthesis and Performance. *ACS Omega* **7**, 21654–21663 (2022).
17. Armor, J. N. A history of industrial catalysis. *Catal Today* **163**, 3–9 (2011).
18. Morris, R. E. & Weigel, S. J. The synthesis of molecular sieves from non-aqueous solvents. *Chem Soc Rev* **26**, 309–317 (1997).
19. Li, J., Corma, A. & Yu, J. Synthesis of new zeolite structures. *Chem Soc Rev* **44**, 7112–7127 (2015).
20. Zukal, A., Patzelova, V. & Lohse, U. Secondary porous structure of dealuminated Y zeolites. *Zeolites* **6**, 133–136 (1986).
21. Čejka, J., Bekkum, H., Corma, A. & Schüth, F. *Introduction to Zeolite Molecular Sieves*. (Elsevier Science, 2007).
22. C. Baerlocher & L.B. McCusker. Database of Zeolite Structures. <http://www.iza-structure.org/databases/>.
23. Cundy, C. S. & Cox, P. A. The Hydrothermal Synthesis of Zeolites: History and Development from the Earliest Days to the Present Time. *Chem Rev* **103**, (2003).
24. Möller, K. & Bein, T. Mesoporosity – a new dimension for zeolites. *Chem Soc Rev* **42**, 3689–3707 (2013).

25. Pang, T. *et al.* Recent advance in synthesis and application of heteroatom zeolites. *Chinese Chemical Letters* **32**, 328–338 (2021).
26. Fecheté, I., Wang, Y. & Védrine, J. C. The past, present and future of heterogeneous catalysis. *Catal Today* **189**, 2–27 (2012).
27. Corma, A. Inorganic Solid Acids and Their Use in Acid-Catalyzed Hydrocarbon Reactions. *Chem Rev* **95**, 559–614 (1995).
28. Peeters, E., Calderon-Ardila, S., Hermans, I., Dusselier, M. & Sels, B. F. Toward Industrially Relevant Sn-BETA Zeolites: Synthesis, Activity, Stability, and Regeneration. *ACS Catal* **12**, 9559–9569 (2022).
29. Busca, G. Acidity and basicity of zeolites: A fundamental approach. *Microporous and Mesoporous Materials* **254**, 3–16 (2017).
30. Boronat, M. & Corma, A. Factors Controlling the Acidity of Zeolites. *Catal Letters* **145**, 162–172 (2015).
31. Boronat, M. & Corma, A. What Is Measured When Measuring Acidity in Zeolites with Probe Molecules? *ACS Catal* **9**, 1539–1548 (2019).
32. Peeters, E., Calderon-Ardila, S., Hermans, I., Dusselier, M. & Sels, B. F. Toward Industrially Relevant Sn-BETA Zeolites: Synthesis, Activity, Stability, and Regeneration. *ACS Catal* **12**, 9559–9569 (2022).
33. Kunkeler, P. J. *et al.* Zeolite Beta: The relationship between calcination procedure, aluminum configuration, and Lewis acidity. *J Catal* **180**, 234–244 (1998).
34. Smit, B. & Maesen, T. L. M. Towards a molecular understanding of shape selectivity. *Nature* **451**, 671–678 (2008).
35. Lobo, R. F., Zones, S. I. & Davis, M. E. Structure-Direction in Zeolite Synthesis. *Springer* 47–78 (1995).
36. Olah, G. A. *et al.* Boron, Aluminum, and Gallium Tris(trifluoromethanesulfonate) (Triflate): Effective New Friedel-Crafts Catalysts. *J Am Chem Soc* **110**, 2560–2565 (1988).

37. Young, L. B., Butter, S. A. & Kaeding, W. W. Shape selective reactions with zeolite catalysts: III. Selectivity in xylene isomerization, toluene-methanol alkylation, and toluene disproportionation over ZSM-5 zeolite catalysts. *J Catal* **76**, 418–432 (1982).
38. Cundy, C. S. & Cox, P. A. The hydrothermal synthesis of zeolites: Precursors, intermediates and reaction mechanism. *Microporous and Mesoporous Materials* **82**, 1–78 (2005).
39. Asselman, K. *et al.* Structural Aspects Affecting Phase Selection in Inorganic Zeolite Synthesis. *Chemistry of Materials* **34**, 11081–11092 (2022).
40. Veselý, O., Morris, R. E. & Čejka, J. Beyond traditional synthesis of zeolites: The impact of germanosilicate chemistry in the search for new materials. *Microporous and Mesoporous Materials* 112385 (2022).
41. Gopal, S., Yoo, K. & Smirniotis, P. G. Synthesis of Al-rich ZSM-12 using TEOH as template. *Microporous and Mesoporous Materials* **49**, 149–156 (2001).
42. Cambor, M. A., Mifsud, A. & Perez-Pariente, J. Influence of the synthesis conditions on the crystallization of zeolite Beta. *Zeolites* **11**, (1991).
43. Liu, X. D., Wang, Y. P., Cui, X. M., He, Y. & Mao, J. Influence of synthesis parameters on NaA zeolite crystals. *Powder Technol* **243**, 184–193 (2013).
44. Corn, R. M. Lecture C4b Microscopic to Macroscopic, Part 4: X-Ray Diffraction and Crystal Packing. (2023).
45. Bunaciu, A. A., Udriștioiu, E. G. & Aboul-Enein, H. Y. X-Ray Diffraction: Instrumentation and Applications. *Taylor and Francis online* **45**, 289–299 (2015).
46. Bunaciu, A. A., Gabriela Udriștioiu, E. & Aboul-Enein, H. Y. Critical Reviews in Analytical Chemistry X-Ray Diffraction: Instrumentation and Applications X-Ray Diffraction: Instrumentation and Applications. *Crit Rev Anal Chem* **45**, 289–299 (2015).
47. Goj, A., Sholl, D. S., Demet Akten, \perp E & Kohen, D. Atomistic Simulations of CO₂ and N₂ Adsorption in Silica Zeolites: The Impact of Pore Size and Shape. *J. Phys. Chem.* (2002).

48. Sing, K. The use of nitrogen adsorption for the characterisation of porous materials. *Colloids and surfaces A* **187**, 3–9 (2001).
49. Thielmann, F. & Burnett, D. DVS Application Note 26 Isotherm Types and Adsorption Mechanisms of Solvents on Pharmaceutical Excipients. (1996).
50. Kumar, K. V. *et al.* Characterization of the adsorption site energies and heterogeneous surfaces of porous materials. *J Mater Chem A Mater* **7**, 10104–10137 (2019).
51. Thommes, M. *et al.* IUPAC Technical Report Physisorption of gases, with special reference to the evaluation of surface area and pore size distribution (IUPAC Technical Report). *Pure Appl. Chem.* (2015).
52. Brunauer, S., Emmett, P. H. & Teller, E. Adsorption of Gases in Multimolecular Layers. *J Am Chem Soc* **60**, 309–319 (1938).
53. Castellà-Ventura, M., Akacem, Y., Kassab, E. & El Beida, D. Vibrational Analysis of Pyridine Adsorption on the Brønsted Acid Sites of Zeolites Based on Density Functional Cluster Calculations.
54. Gil, B., Zones, S. I., Hwang, S. J., Bejblová, M. & Čejka, J. Acidic properties of SSZ-33 and SSZ-35 novel zeolites: A complex infrared and MAS NMR study. *Journal of Physical Chemistry C* **112**, 2997–3007 (2008).
55. Jentys, A. & Lercher, J. A. Chapter 8 Techniques of zeolite characterization. *Stud Surf Sci Catal* **137**, 345–386 (2001).
56. Lopez-Orozco, S., Inayat, A., Schwab, A., Selvam, T. & Schwieger, W. Zeolitic Materials with Hierarchical Porous Structures. *Advanced Materials* **23**, 2602–2615 (2011).
57. Roduner, E. Understanding catalysis †. *Chem Soc Rev* **43**, 8226 (2014).
58. Laursen, A. B., Man, I. C., Trinhammer, O. L., Rossmeisl, J. & Dahl, S. The Sabatier principle illustrated by catalytic H₂O₂ decomposition on metal surfaces. *J Chem Educ* **88**, 1711–1715 (2011).
59. Bartle, K. D. & Myers, P. History of gas chromatography. *TrAC Trends in Analytical Chemistry* **21**, 547–557 (2002).

60. Čejka, J., Centi, G., Perez-Pariente, J. & Roth, W. J. Zeolite-based materials for novel catalytic applications: Opportunities, perspectives and open problems. *Catal Today* **179**, 2–15 (2012).
61. Maxwell, I. E. Zeolite catalysis in hydroprocessing technology. *Catal Today* **1**, 385–413 (1987).
62. Blauwhoff, P. M. M., Gosselink, J. W., Kieffer, E. P., Sie, S. T. & Stork, W. H. J. Zeolites as Catalysts in Industrial Processes. *Catalysis and Zeolites* 437–538 (1999).
63. Martínez, C. & Corma, A. Inorganic molecular sieves: Preparation, modification and industrial application in catalytic processes. *Coord Chem Rev* **255**, 1558–1580 (2011).
64. Vogt, E. T. C. & Weckhuysen, B. M. Fluid catalytic cracking: recent developments on the grand old lady of zeolite catalysis. *Chem Soc Rev* **44**, 7342–7370 (2015).
65. Vogt, E. T. C., Whiting, G. T., Dutta Chowdhury, A. & Weckhuysen, B. M. Zeolites and Zeotypes for Oil and Gas Conversion. *Advances in Catalysis* **58**, 143–314 (2015).
66. Vermeiren, W. & Gilson, J. P. Impact of zeolites on the petroleum and petrochemical industry. *Top Catal* **52**, 1131–1161 (2009).
67. Ennaert, T. *et al.* Potential and challenges of zeolite chemistry in the catalytic conversion of biomass. *Chem Soc Rev* **45**, 584–611 (2016).
68. Serrano, D. P., Melero, J. A., Morales, G., Iglesias, J. & Pizarro, P. Progress in the design of zeolite catalysts for biomass conversion into biofuels and bio-based chemicals. *Catalysis Reviews* **60**, 1–70 (2018).
69. Moliner, M. State of the art of Lewis acid-containing zeolites: lessons from fine chemistry to new biomass transformation processes. *Dalton Transactions* **43**, 4197–4208 (2014).
70. Martínez, C. & Corma, A. Inorganic molecular sieves: Preparation, modification and industrial application in catalytic processes. *Coord Chem Rev* **255**, 1558–1580 (2011).
71. Ennaert, T. *et al.* Potential and challenges of zeolite chemistry in the catalytic conversion of biomass. *Chem Soc Rev* **45**, 584–611 (2016).

72. Opanasenko, M. V., Roth, W. J. & Čejka, J. Two-dimensional zeolites in catalysis: current status and perspectives. *Catal Sci Technol* **6**, 2467–2484 (2016).
73. Přeč, J., Pizarro, P., Serrano, D. P. & Čejka, J. From 3D to 2D zeolite catalytic materials. *Chem Soc Rev* **47**, 8263–8306 (2018).
74. Dartt, C. B. & Davis, M. E. Chapter 6 Applications of zeolites to fine chemicals synthesis. *Catal Today* **19**, 151–186 (1994).
75. Grant, H. G. & Summers, L. A. Synthesis of N-methyl-N-(2,2,2-trichloro-1-arylaminoethyl)formamides and related compounds as potential fungicides. *Aust J Chem* **33**, 613–617 (1980).
76. Jackson, A. & Meth-Cohn, O. A new short and efficient strategy for the synthesis of quinolone antibiotics. *J Chem Soc Chem Commun* 1319–1319 (1995).
77. Pettit, G. R., Kalnins, M. V., Liu, T. M. H., Thomas, E. G. & Parent, K. Potential Cancerocidal Agents. III. Formanilides. *Journal of Organic Chemistry* **26**, 2563–2566 (1961).
78. Chandra Shekhar, A. *et al.* Facile N-formylation of amines using Lewis acids as novel catalysts. *Tetrahedron Lett* **50**, 7099–7101 (2009).
79. Dai, X. *et al.* Supported CuII Single-Ion Catalyst for Total Carbon Utilization of C2 and C3 Biomass-Based Platform Molecules in the N-Formylation of Amines. *Chemistry – A European Journal* **27**, 16889–16895 (2021).
80. Bhat, S. U., Naikoo, R. A. & Kumar, N. Synthesis of N-Formylation of Amines using Various Ion Exchanged Forms of Zeolite-A as Catalysts. *Pharm Pharmacol Int J* **5**, (2017).
81. Nasrollahzadeh, M., Sajadi, S. M. & Hatamifard, A. Anthemis xylopoda flowers aqueous extract assisted in situ green synthesis of Cu nanoparticles supported on natural Natrolite zeolite for N-formylation of amines at room temperature under environmentally benign reaction conditions. *J Colloid Interface Sci* **460**, 146–153 (2015).

82. Tajbakhsh, M., Alinezhad, H., Nasrollahzadeh, M. & Kamali, T. A. Preparation, characterization and application of nanosized CuO/HZSM-5 as an efficient and heterogeneous catalyst for the N-formylation of amines at room temperature. *J Colloid Interface Sci* **471**, 37–47 (2016).
83. Barakov, R. *et al.* Hierarchical Beta zeolites obtained in concentrated reaction mixtures as catalysts in tetrahydropyranylation of alcohols. *Appl Catal A Gen* **594**, (2020).
84. Zholobenko, V. *et al.* Probing the acid sites of zeolites with pyridine: Quantitative AGIR measurements of the molar absorption coefficients. *J Catal* **385**, 52–60 (2020).
85. Zu, Y. *et al.* Investigation of Cu(I)-Y zeolites with different Cu/Al ratios towards the ultra-deep adsorption desulfurization: Discrimination and role of the specific adsorption active sites. *Chemical Engineering Journal* **380**, 122319 (2020).